ARMY RESEARCH LABORATORY

Viscoelastic Properties of Alkoxy Silane-Epoxy Interpenetrating Networks

by Robert E. Jensen, Steven H. McKnight, and Giuseppe R. Palmese

ARL-TR-3109 **November 2003**

NOTICES

Disclaimers

The findings in this report are not to be construed as an official Department of the Army position unless so designated by other authorized documents.

Citation of manufacturer's or trade names does not constitute an official endorsement or approval of the use thereof.

Destroy this report when it is no longer needed. Do not return it to the originator.

Army Research Laboratory

Aberdeen Proving Ground, MD 21005-5069

Viscoelastic Properties of Alkoxy Silane-Epoxy Interpenetrating Networks

Robert E. Jensen and Steven H. McKnight
Weapons and Materials Research Directorate, ARL

Giuseppe R. Palmese
Center for Composite Materials, University of Delaware

Report Documentation Page

Form Approved
OMB No. 0704-0188

Public reporting burden for this collection of information is estimated to average 1 hour per response, including the time for reviewing instructions, searching existing data sources, gathering and maintaining the data needed, and completing and reviewing the collection information. Send comments regarding this burden estimate or any other aspect of this collection of information, including suggestions for reducing the burden, to Department of Defense, Washington Headquarters Services, Directorate for Information Operations and Reports (0704-0188), 1215 Jefferson Davis Highway, Suite 1204, Arlington, VA 22202-4302. Respondents should be aware that notwithstanding any other provision of law, no person shall be subject to any penalty for failing to comply with a collection of information if it does not display a currently valid OMB control number. **PLEASE DO NOT RETURN YOUR FORM TO THE ABOVE ADDRESS.**

1. REPORT DATE *(DD-MM-YYYY)*	2. REPORT TYPE	3. DATES COVERED *(From - To)*
November 2003	Final	September 1999 - May 2001

4. TITLE AND SUBTITLE	5a. CONTRACT NUMBER
Viscoelastic Properties of Alkoxy Silane-Epoxy Interpenetrating Networks	DAAD19-01-2-0001
	5b. GRANT NUMBER
	5c. PROGRAM ELEMENT NUMBER

6. AUTHOR(S)	5d. PROJECT NUMBER
Robert E. Jensen, Steven H. McKnight, and Giuseppe R. Palmese*	AH42
	5e. TASK NUMBER
	5f. WORK UNIT NUMBER

7. PERFORMING ORGANIZATION NAME(S) AND ADDRESS(ES)	8. PERFORMING ORGANIZATION REPORT NUMBER
U.S. Army Research Laboratory ATTN: AMSRL-WM-MA Aberdeen Proving Ground, MD 21005-5069	ARL-TR-3109

9. SPONSORING/MONITORING AGENCY NAME(S) AND ADDRESS(ES)	10. SPONSOR/MONITOR'S ACRONYM(S)
	11. SPONSOR/MONITOR'S REPORT NUMBER(S)

12. DISTRIBUTION/AVAILABILITY STATEMENT

Approved for public release; distribution is unlimited.

13. SUPPLEMENTARY NOTES

*Center for Composite Materials, University of Delaware, Newark, DE 19716

14. ABSTRACT

A model epoxy-silane interpenetrating network (IPN) was synthesized to simulate the molecular structure found at the fiber-matrix interphase. The Young's modulus (E) of the epoxy-silane IPN was determined through micromechanical analysis both quasi-statically and in the frequency domain. The epoxy-silane IPN was synthesized by diffusion of uncured diglycidyl ether of bisphenol A (DGEBA) epoxy resin and bis (*p*-aminocyclohexyl) methane (PACM) curing agent into spherical particles of condensed and crosslinked 3-glycidoxypropyltrimethoxysilane (GPS). This IPN composition was chosen to simulate the typical properties of a silane modified interphase found in glass reinforced composites. Differential scanning calorimetry showed that the glass transition temperature (T_g) of the initial crosslinked siloxane network increased upon cure of the DGEBA and PACM, but was still significantly lower than that of the neat epoxy matrix. Additionally, dynamic mechanical analysis was used in conjunction with the micromechanical C-Combining Rule to show that the Young's modulus of the epoxy-silane IPN spherical inclusions (E_i) was decreased in comparison to the Young's modulus of the matrix epoxy (E_m) at all temperatures. The time-temperature superposition (tTsp) principle was successfully applied to the epoxy-silane IPN to determine viscoelastic properties at high frequencies. The viscoelastic properties of the epoxy-silane IPN may have implications with respect to the ballistic impact resistance of composite structures used for U.S. Army applications.

15. SUBJECT TERMS

interphase, silane, IPN, modulus, viscoelasticity, epoxy, amine, composite, adhesion

16. SECURITY CLASSIFICATION OF:			17. LIMITATION OF ABSTRACT	18. NUMBER OF PAGES	19a. NAME OF RESPONSIBLE PERSON
					Robert E. Jensen
a. REPORT	b. ABSTRACT	c. THIS PAGE	UL	40	19b. TELEPHONE NUMBER *(Include area code)*
UNCLASSIFIED	UNCLASSIFIED	UNCLASSIFIED			410-306-1910

Standard Form 298 (Rev. 8/98)
Prescribed by ANSI Std. Z39.18

Contents

List of Figures

List of Tables

Acknowledgments

1. Introduction

The role of silane coupling agents on adhesion promotion between polymers and inorganic surfaces has been widely documented. Much attention has been placed on the specific interaction of alkoxy and chloro silane species with adherend surfaces (*1–5*). Another large body of research has focused on the interaction and reaction of the organic functional group of the silane coupling agent with the matrix polymer (*6–8*). It is also widely recognized that, in application, the adsorbed silane usually exists as a surface-tethered crosslinked network of varied thickness. The three-dimensional interphase (figure 1) is created by interdiffusion and chemical reactions between the polymer matrix and silane layer, subsequently forming an interpenetrating network (IPN) type of molecular architecture in the fiber-matrix interphase region (*9, 10*). While many have noted the role of subsequent diffusion and/or chemical reaction of the polymer resin within the multilayer silane network, very little research has been performed to characterize the nature of the structure and properties of this interphase material (*11, 12*).
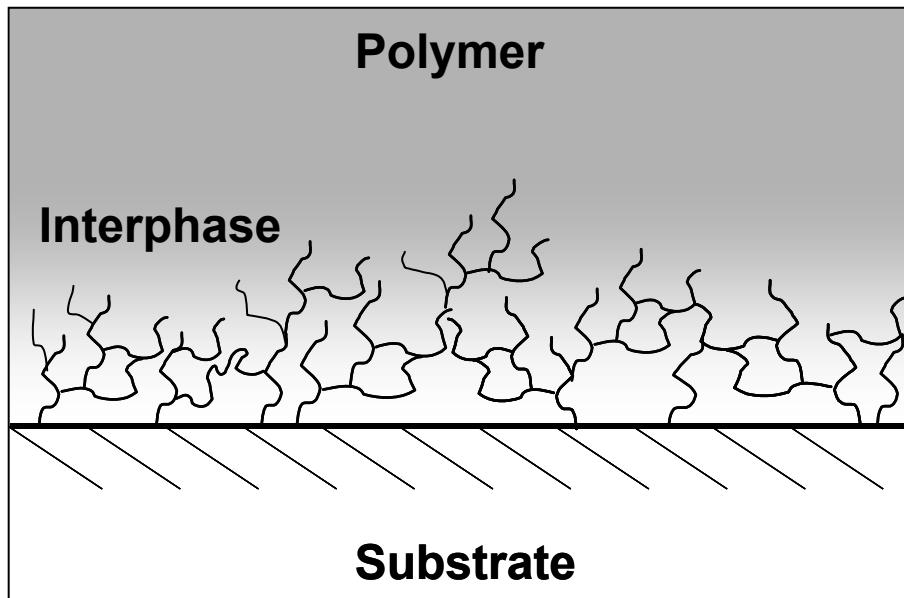
Figure 1. Schematic of polymer-matrix interphase.

Many resulting adhesive bonding properties may be directly affected by the nature of this interphase network structure. For example, it is well known that the fiber-matrix interphase plays the most critical role with respect to the micromechanical failure mechanisms and hygro-thermal resistance that govern the overall durability of glass fiber reinforced composites (*13–16*). The adhesive bond strength of the interphase also influences the ballistic properties of

composites used in lightweight armor applications (*17*). The time- and temperature-dependent mechanical properties (modulus, Poisson's ratio, etc.) of the interphase network may also strongly influence these aspects of composite performance. Indeed, recent research has shown that a rate dependence on the response of the fiber-matrix interphase can be observed during fiber push-out tests (*18*). This research also revealed that the rate dependence of the initial fiber-matrix loading and failure was related to the type of silane-based sizing package applied to the glass fiber. However, the role of the complicated polymer network structure that is formed near the solid fiber surface with respect to rate-dependent composite properties is largely unknown.

Previous attempts to quantify the mechanical properties of the fiber-matrix interphase in composite materials using techniques such as atomic force microscopy and dynamic mechanical analysis (DMA) have not been successful due to the small volume fraction (V_f) of material located in the interphase region as well as possible fiber artifacts governing the interphase mechanical response (*19–21*). An alternative approach to elucidate the properties of interphase materials by studying model epoxy-silane networks purposely formed in the absence of a fiber surface has been recently reported (*22*). Model interphase materials were synthesized to simulate commercial-based silane glass fiber sizings, which were subsequently confirmed to match their commercial counterparts in chemical composition via nuclear magnetic resonance (NMR) spectroscopy. The primary advantage of synthesizing a model interphase material is that large volume fractions ($V_f \sim 0.50$) can then be incorporated into a matrix resin as micro-sized spherical inclusions to form particulate filled composites. During processing, the unreacted matrix resin monomers diffuse into the inclusions and react with each other and the organo-functional groups of the siloxane network to form an IPN morphology upon cure. The material properties of the model interphase IPN can then be determined via the mechanical characterization of the model particulate filled composites and suitable application of traditional micromechanics.

The present study is focused on determining the quasi-static and viscoelastic mechanical properties of a model epoxy-silane IPN that is representative of the interphase region formed between a silane surface bound to a glass fiber and a thermosetting resin (e.g., glass-fiber epoxy composite materials). The experimental technique developed by Tanoglu et al. (*22*), which is outlined schematically in figure 2, is further expanded to investigate the frequency-dependent viscoelastic properties of the model epoxy-silane IPN using DMA. The model IPN was chosen to simulate the polymeric fiber-matrix interphase microstructure found in typical glass-reinforced composites. Micromechanical models were used to analyze the results of DMA experiments on a series of model particulate filled composite specimens (epoxy-silane IPN inclusions in an epoxy matrix) and used to quantify the viscoelastic properties of the embedded epoxy-silane IPN. These results point to the role of the IPN on the properties of epoxy-silane interphase structures typical of those found in composite materials and other silane-modified bonds.
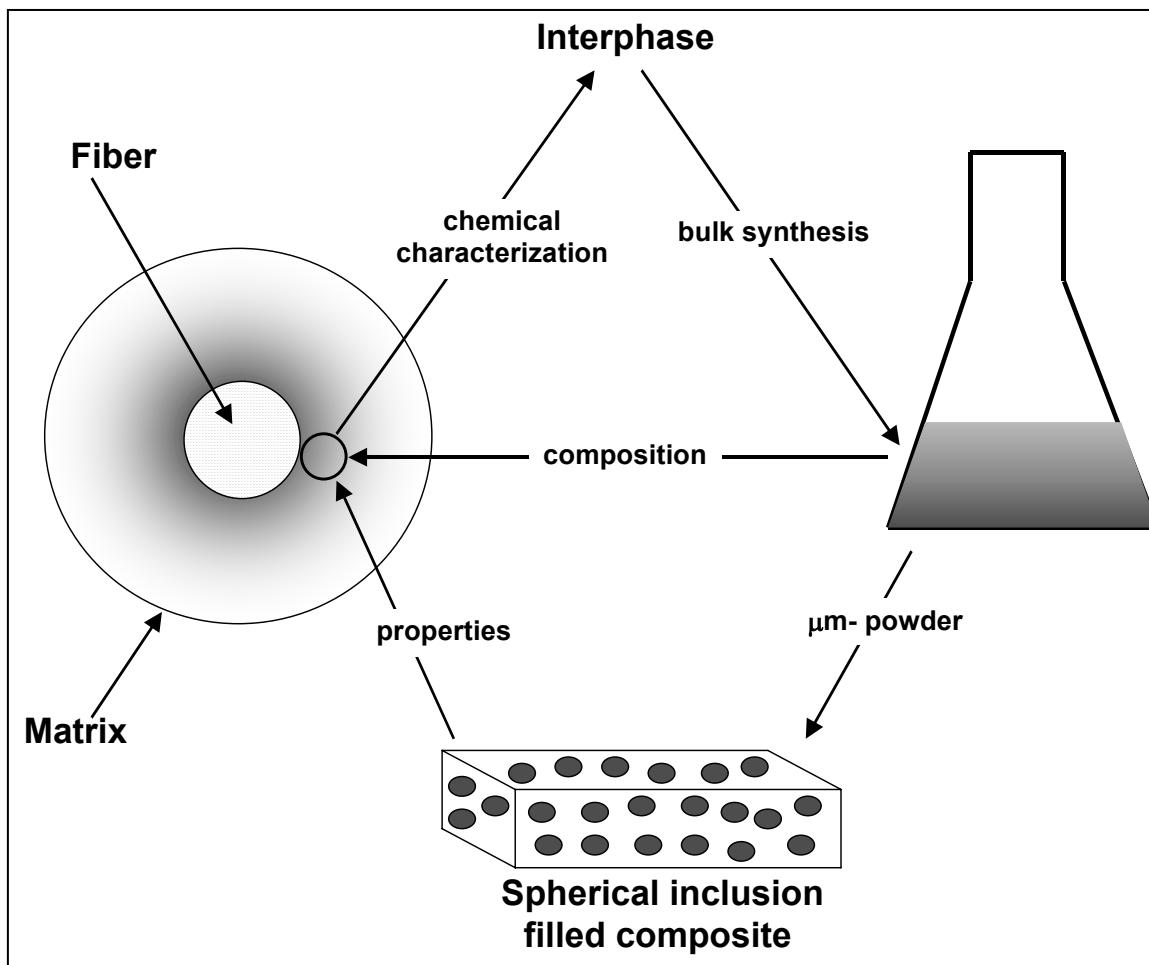
Figure 2. Schematic outline of approach used to characterize interphase properties.

2.   Experimental and Analysis

2.1   Materials

The IPN constituent materials used in this study were composed of a matrix resin and a model silane-based sizing compound. The matrix resin consisted of diglycidyl ether of bisphenol A (DGEBA EPON 828) obtained from the Shell Chemical Company. The DGEBA resin was cured with stoichiometric amounts of bis (*p*-aminocyclohexyl) methane (PACM), which was acquired from Air Products and Chemical, Incorporated. The model sizing material used was intended to mimic typical glass fiber sizing formulations used commercially, and contained 3-glycidoxypropyltrimethoxysilane (GPS) (Dow Corning Corporation Z-6040). The initial synthesis step of the model-sizing material preparation also included the incorporation of a water-based dispersion of high molecular weight DGEBA film former, which was emulsified using a nonionic polyethylene oxide-polypropylene oxide-polyethylene oxide (PEO-PPO-PEO)

triblock copolymer surfactant. The Owens Corning Company generously provided the film former emulsion. A detailed chemical and solids analysis is provided elsewhere (*22*). Chemical structures of the matrix epoxy, amine curing agent, and silane coupling agent are provided in figure 3.
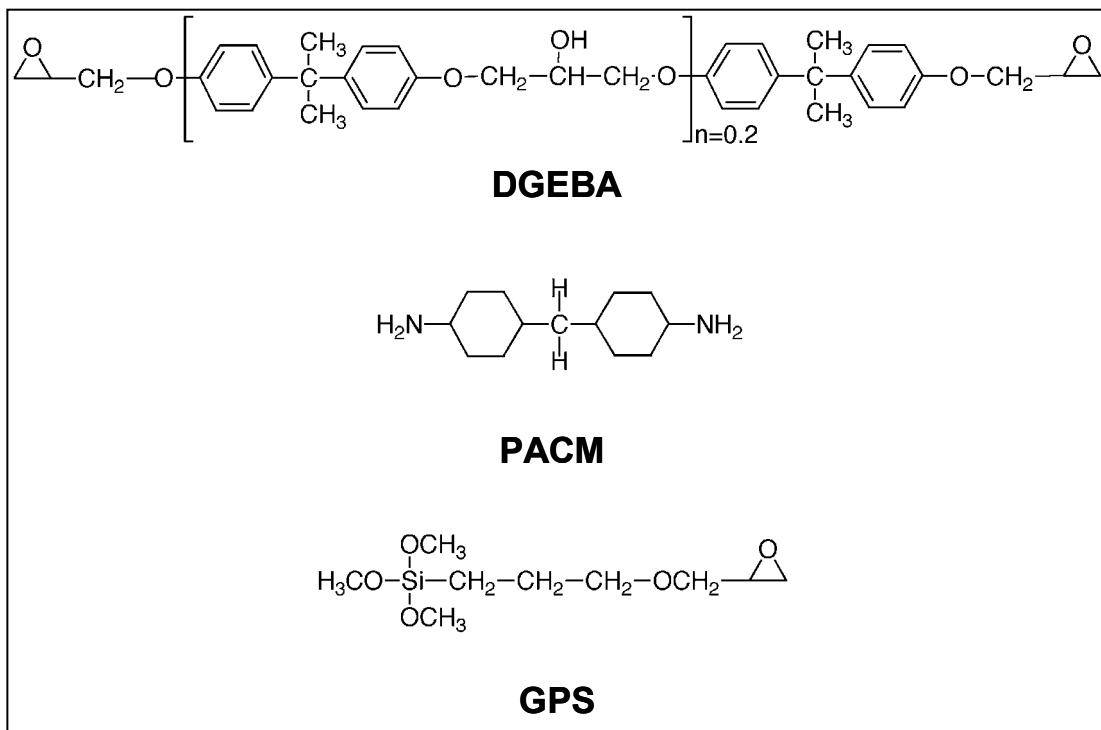
Figure 3. Matrix epoxy, curing agent, and silane coupling agent.

2.2   Bulk Silane Powder Synthesis and Blend Processing

The objective of this research is to determine the properties of a model interphase of typical commercially treated glass fiber composites, thus the incorporation of film former and surfactant into the formulation. Processing of the sizing formulation proceeded in a manner similar to commercial treatment of glass fibers except that the sizing was allowed to condense and crosslink in the absence of any glass surface. A 10 weight-percent solution of GPS in distilled water (pH adjusted to 4.5 with acetic acid to promote hydrolysis of the silane) is added to the film former emulsion in a ratio to yield 15 weight-percent solids upon evaporation of the aqueous phase. This evaporation was carried out in a forced air convection oven at a temperature of 65 °C over a period of time of several days to allow for the condensation and crosslinking of the silane coupling agent. The soluble portions of the dried solids are removed using a Soxhlet extraction procedure in acetone, which has a similar solubility parameter (δ) to the DGEBA epoxy resin, $\delta_{acetone} = 20.3$ $(J/cm^3)^{1/2}$ vs. $\delta_{DGEBA} = 21.1$ $(J/cm^3)^{1/2}$ (*23*). Upon completion of solubles extraction, a gelled insoluble silane powder remains. The insoluble silane powder has a composition of 73% crosslinked GPS, 19% surfactant, and 8% film former by

4

weight, which is very comparable to what is found on the surface of commercially treated fibers after similar extraction experiments (*22, 24*).

Particle size distributions of the crosslinked silane powder were measured using a Horiba Instruments LA 900 light-scattering particle-size analyzer. The particle-size analysis, illustrated in figure 4, displayed bimodal distributions, with the larger particle sizes attributed to agglomeration. The average particle size measured using water as the dispersing medium was 1.9 μm. When acetone was substituted as the dispersing medium significant swelling was observed and the average particle size increased to 7.2 μm, including a substantial increase in the larger particle diameter portion of the distribution plots.
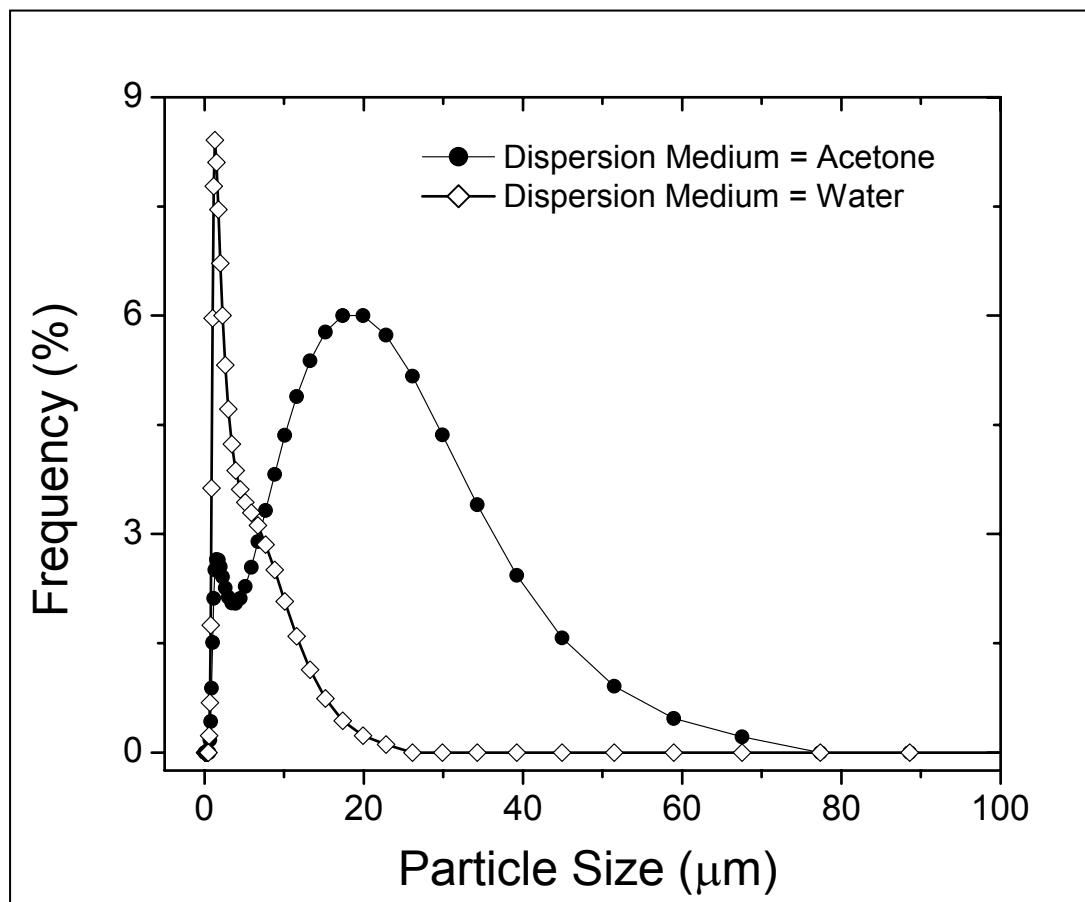
Figure 4. Particle size distributions of bulk condensed and crosslinked silane particles prior to incorporation into the epoxy matrix. Particle size varied with dispersion solvent (water vs. acetone shown).

The bulk silane powder was then dispersed into the epoxy-amine matrix at high-volume fractions using a high-speed/high-shear mixer. The unreacted epoxy-bulk silane mixtures were degassed under vacuum, cast into rectangular high-temperature silicone molds, and thermally cured at 80 °C for 2 hr and post-cured at 160 °C for 1 hr. Under these curing conditions, the time for diffusion ($t_{\text{diffusion}}$) of resin/curing agent into the inclusion is much less than the time for reaction

($t_{reaction}$). The diffusion of the resin/curing into the silane inclusions to form dispersed particles of epoxy-silane IPN material was verified by studying the matrix epoxy T_g while varying the matrix amine:epoxy stoichiometry ratio, which is discussed further in the experimental results section. Upon completion of the post-cure step, the oven was allowed to slow-cool overnight to minimize residual cure stresses. A scanning electron microscopy (SEM) image of a cross section of the epoxy-silane IPN inclusions embedded in the cured epoxy matrix is illustrated in figure 5.
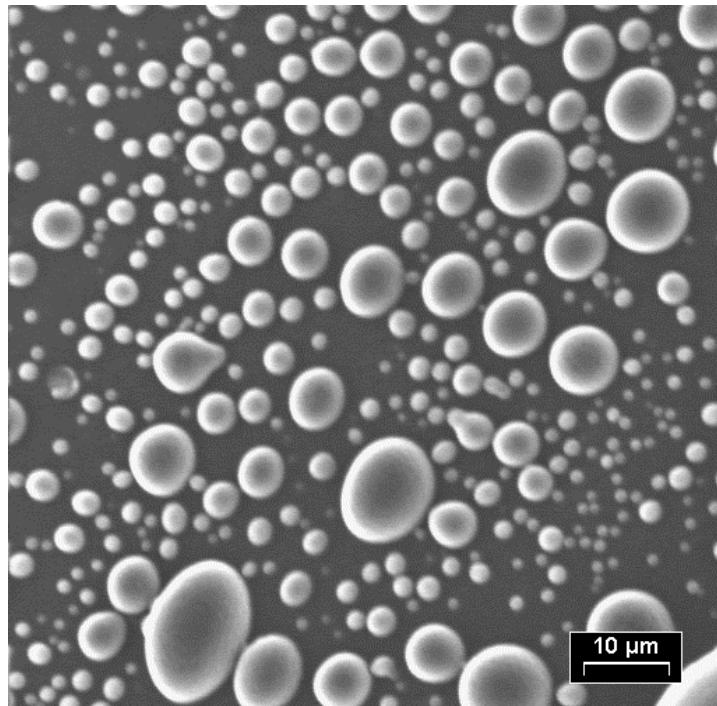
Figure 5. SEM cross section of epoxy-silane IPN inclusion filled composite showing spherical IPN particles embedded in the cured and glassy epoxy matrix.

The static tensile Young's moduli of the neat epoxy matrix (E_m) and epoxy-silane IPN particulate filled composites (E_c) were measured in a 3-point bending mode configuration using an Instron tensile testing instrument. Rectangular samples were prepared with dimensions of width, thickness, and length provided by the recommended guidelines listed in ASTM D 790-96a (*25*) to ensure that the proper support span-to-depth ratio was maintained. A bending mode was used to measure E_m and E_c statically because a similar oscillatory configuration could be used in DMA. Dynamic mechanical analysis was carried out using a TA Instruments 2980 DMA with a 20-mm dual cantilever clamp frame. The samples were tested at an oscillatory displacement amplitude of 7.5 μm. The displacement amplitude was verified to ensure linear viscoelastic response by deriving corresponding stress-strain (σ-ε) curves. Constant heating rate experiments were carried out at 2.0 °C/min at a frequency of 1 Hz from −135 to 225 °C. Master curves were constructed from data obtained from multiple frequency sweeps, which were measured over three decades of frequency (0.1, 0.3, 1, 3, 10, and 30 Hz) in 3 °C isothermal steps. The

α and β transition temperatures were taken as the peak maximum of the loss modulus (E'') curves measured at 1 Hz. The glass transition temperatures (T_g) of the cured samples were also measure using a TA Instruments 2980 differential scanning calorimetry (DSC) at a heating rate of 15 °C/min.

2.3 Micromechanical Analysis

Micromechanical combining rules can be used to describe the elastic and viscoelastic behavior of a polymer composite using constituent properties and compositional information. With some effort these rules can be used to determine constituent properties from composite measurements. Thus, by measuring the properties of the model epoxy-silane IPN particulate filled composite and the matrix epoxy, the unknown properties of the epoxy-silane IPN spherical inclusions can be determined.

In this work, we selected the C-Combining Rule (equation 1) as our model. The C-Combining Rule can predict properties of composites (P_c) filled with spherically shaped particulate inclusions based upon knowledge of the volume fractions (V), Poisson's ratios (ν), properties (P) of the matrix (m), and inclusion (i) phases (*26*).

$$P_c = V_m P_u + V_i P_l + \lambda_p V_i V_m (P_u - P_l),\qquad(1)$$

where

$$P_u = P_m \left(1 - \left[\frac{V_i(P_m - P_i)}{P_m - V_m(P_m - P_i)\eta_{Pm}}\right]\right),\qquad(2)$$

$$P_l = P_i \left(1 + \left[\frac{V_m(P_m - P_i)}{P_i - V_i(P_m - P_i)\eta_{Pi}}\right]\right),\qquad(3)$$

and

$$\lambda_p = \frac{2\phi_c - 1}{\phi_c\left[1 - 2\phi_c(1 - \phi_c)\eta_{Pm}\right]}.\qquad(4)$$

The C-Combining Rule uses the Hashin and Shtrikman (*27*) improved upper (P_u) and lower bounds (P_l) and incorporates a phase contiguity parameter (λ_p). The term ϕ_c represents a critical packing volume fraction, which for the case of simple spherical packing ϕ_c is equal to 0.74. Equations 5 and 6 define the term η_{Pj}, where $j = i$ or m.

$$\eta_{Kj} = \frac{3K_j}{3K_j + 4G_j} = \frac{1 + \nu_j}{3(1 - \nu_j)};\qquad(5)$$

$$\eta_{Gj} = \frac{6(K_j + 2G_j)}{5(3K_j + 4G_j)} = \frac{2(4 - 5\nu_j)}{15(1 - \nu_j)}.\qquad(6)$$

The C-Combining Rule, as is the case for most predictive modulus relationships, is only rigorously correct for either bulk modulus (K) or shear modulus (G). The Young's modulus, which is more dependent upon Poisson's ratio, is derived using equations 7 and 8.

$$E = \frac{9KG}{3K + G};$$ (7)

$$v = \frac{3K - 2G}{2(3K + G)}.$$ (8)

Thus, by measuring the global properties of the composites that include epoxy-silane IPN inclusions as well as the properties of the cured matrix resin, the C-Combining Rule can be used to "back-out" the actual epoxy-silane IPN inclusion properties. While simple in theory, the application of the C-Combining Rule, due to the numerous embedded equations (equations 2–8), can be very time consuming when multiple data sets must be evaluated (e.g., DMA runs with several tens of curves at several different frequencies). One may wish to employ a more convenient approximation of equation 1 for analysis of modulus data.

One can show from equations 7 and 8 that the C-Combining Rule can be expressed as the ratio E_c/E_m in the following exponential series expansion form:

$$\frac{E_c}{3E_m} = H = \left[H_0 - \frac{1}{2}\left(\frac{\mu'}{\mu^2}\right)(1 - Z) \right]\exp^Z + \frac{1}{2}\left(\frac{\mu'}{\mu^2}\right) + \dots ;$$ (9)

$$Z = H_0\mu_0'\left(V_i - V_i^*\right);$$ (10)

$$\mu = -\left(2(1 + v_m)\left(\frac{G_m - G_i}{G_m}\right) + (1 - 2v_m)\left(\frac{K_m - K_i}{K_m}\right) \right).$$ (11)

The series expansion shown equation 9 can be used to solve for E_i by defining E_c in terms of E_i and E_m through any micromechanical model. The expansion is then solved about an arbitrary reference volume fraction (V_i^*) with $H_0 = \mu_0'$ at $V_i = V_i^*$. Determination of E_c in terms of E_i and E_m through the C-Combining Rule and subsequent substitution into equation 9 yields a 6th-order polynomial solution set for E_i. Although a physical interpretation of equation 9 through more complicated micromechanical models is difficult, it can be seen that a simple exponential fitting expression may be used to approximate the rigorous exponential series expansion derived in equation 9. Hence it may be convenient to approximate the C-Combining Rule as follows:

$$\frac{E_c}{E_m} = \exp\left[-bV_i\right],$$ (12)

where b captures the terms in equations 10 and 11. This approximation greatly simplifies the following viscoelastic analysis of the composite specimens.

Dickie (*28*) and Schapery (*29*) have shown that the imaginary term of the complex modulus (E^*) must be carried through combining rule analysis of polymer blends in the case of a viscoelastic inclusion surrounded by a viscoelastic matrix.

$$E^* = E' + iE''.$$ (13)

If the imaginary term of equation 13 is carried through the combining rule analysis of E_i, then the difficulty of the equation manipulation increases substantially. Fortunately, it can be proved that the imaginary component of E^* can be disregarded from the modulus calculations through the following relationships:

$$\frac{E_i^*}{E_m^*} = \frac{E_i' + iE_i''}{E_m' + iE_m''} = \frac{\left(E_i' + iE_i''\right)\left(E_m' - iE_m''\right)}{E_m'^2 + E_m''^2};$$ (14)

$$\tan\delta_i = \frac{E_i''}{E_i'}, \tan\delta_m = \frac{E_m''}{E_m'};$$ (15)

$$\frac{E_i^*}{E_m^*} = \frac{E_i'}{E_m'}\frac{\left(1 + \tan\delta_i \tan\delta_m\right)}{\left(1 + \left(\tan\delta_m\right)^2\right)}\left(1 + i\left(\tan\left(\delta_i - \delta_m\right)\right)\right).$$ (16)

Therefore, based on the derivation of equation 16, the imaginary component of E^* can be dropped from the ratio of the complex modulus of the inclusion to matrix if the difference in magnitude between the loss tangent (tan δ) signals is small. Additionally, if the tan δ values of the matrix and inclusion are each small then the remaining tan δ coefficients of equation 16 reduce to unity, which leaves the complex modulus ratio approximately equal to the storage modulus ratio. Therefore E' from DMA can be directly substituted for E in equation 12 to give the following expression:

$$\frac{E_c'}{E_m'} = \exp\left[-bV_i\right],$$ (17)

where $E_i' = E_c'$ at an extrapolated volume fraction of $V_i = 1$.

3. Discussion and Results

3.1 Diffusion Time vs. Reaction Time

A primary assumption of this approach is that the chemistry of the model epoxy-silane IPN closely resembles the interphase in actual fiber-reinforced composites. The average particle diameter of the epoxy-silane IPN spherical inclusions is much greater than the length scale of the interphase actually found in a fiber-reinforced composite. It is also known that $t_{\text{diffusion}}$ for the matrix resin and curing agent into the fiber sizing with subsequent equilibration and reaction can

9

occur rapidly (*30*). This raises the question of whether or not the DGEBA and PACM can adequately diffuse into the larger condensed and crosslinked bulk silane spherical inclusions to form a true epoxy-silane IPN structure prior to reaching the gel point of the matrix epoxy phase. Fortunately, a simple verification of the assumption $t_{\text{diffusion}} \ll t_{\text{reaction}}$ can be made by measuring the glass transition temperature (T_g) of the matrix epoxy phase in highly loaded particulate filled composites as a function of amine to epoxy stoichiometry ratios. The T_g of cured DGEBA-PACM epoxy resin is a strong function of reaction stoichiometry and peaks near 160 °C at an amine to epoxy ratio of 1:1 (*31*). Additional PACM was added during the processing of the epoxy-silane IPN particulate filled composites to account for the excess epoxide functional groups of the GPS and film former found in the condensed and crosslinked bulk silane powder. For example, if the particulate filled composite is comprised of 45 weight-percent bulk silane powder then the amine to epoxy ratio of the matrix epoxy phase must be adjusted to 1.3:1 prior to blending to compensate for the additional reactivity of the bulk silane powder toward the PACM curing agent. This formulation is based on a measured epoxy equivalent weight of 500 g/eq (determined via titration and NMR spectroscopy) for the bulk silane powder (*22*). Epoxy-silane IPN particulate filled composite test specimens were prepared with global amine to epoxy ratios of 0.9:1, 1:1, and 1.1:1 (these ratios include the epoxide groups present in the bulk silane powder and matrix epoxy), which yielded matrix epoxy T_g's of 139.5, 155.1, and 152.3 °C, respectively, as measured by DSC. The T_g of the matrix epoxy in the composite samples peaked for the global 1:1 amine to epoxy stoichiometry. If the DGEBA and PACM were not diffusing, swelling, and chemically reacting with the bulk silane filler then a surplus of PACM would remain in the matrix phase, leading to a depressed T_g for the matrix phase. It was determined by DSC that if none of the extra compensatory PACM added to the matrix epoxy resin diffused into and reacted with the bulk silane powder filler to form an epoxy-silane IPN that the matrix epoxy T_g would be depressed to 130 °C. Therefore, based upon the study of T_g vs. amine-to-epoxy stoichiometry measurements, the assumption that the average bulk silane powder diameter was small enough to allow for adequate penetration of a high proportion of the DGEBA and PACM prior to gelation of the matrix phase seems reasonable.

3.2   Epoxy-Silane IPN Structure

The results obtained in this research demonstrate the dramatic changes to network properties as the matrix resin and curing agent diffuse into and cure with the crosslinked silane powder to form an epoxy-silane IPN. Figure 6 shows the DSC results for the bulk silane powder before and also after incorporation into the epoxy matrix to form the particulate filled composite consisting of epoxy-silane IPN inclusions embedded in the epoxy matrix. The virgin bulk silane powder (top curve of figure 6) is compliant at room temperature and has a relatively broad glass-to-rubber transition with a T_g of ~ −50 °C. Unfortunately, the cooling capability of the DSC is realized near −60 °C; therefore, the glass-to-rubber transition of the bulk silane powder
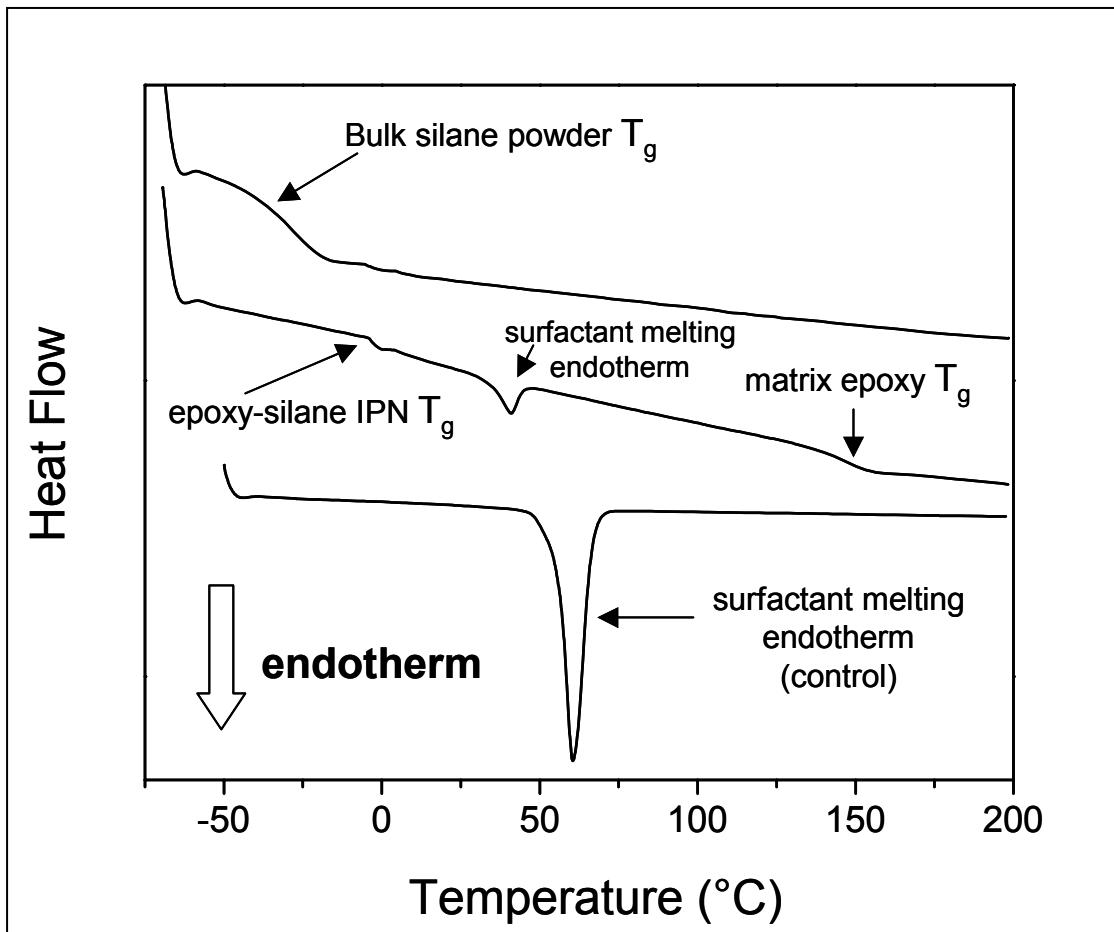
Figure 6. DSC results for nonreacted bulk silane powder (top curve), epoxy-silane IPN inclusion composite ($V_i = 0.49$, center curve), and neat PEO-PPO-PEO triblock copolymer surfactant (bottom curve).

begins as soon as the temperature of the instrument is ramped. The T_g of the epoxy-silane IPN is increased to ~0 °C (indicated in the center trace of figure 6) after diffusion and reaction of the epoxy-amine matrix into the bulk silane powder filler. The additional network coupling reactions of the epoxy organofunctional groups of the silane with the PACM curing agent forms epoxy-silane IPN inclusions with increased crosslink density (ρ_c) in comparison to the bulk silane powder, containing only siloxane crosslinks, which correspondingly increase the T_g of the epoxy-silane IPN in comparison to the initial bulk silane powder. The T_g of the matrix-epoxy resin is observed near 155 °C. The magnitudes of the endothermic glass-to-rubber transitions are decreased for the particulate filled composite due to decreased volume fractions of constituent material present in the sample.

The DSC results also showed a small endothermic peak with an onset near 35 °C, attributed to the melt transition of the block copolymer surfactant, which was transported into the particulate filled composite from within the initial loading of bulk silane powder. For comparison, figure 6 also shows the melt transition of a neat PEO-PPO-PEO triblock copolymer surfactant (BASF

Pluronic F-108), which is a typical representative surfactant used to prepare a commercial-grade aqueous film former dispersion. A rough estimate of the amount of the phase-separated surfactant can be calculated if the melt energy is assumed to be equal to the BASF surfactant (141.7 J/g). The melt energy for the endothermic peak recorded in the epoxy-silane powder inclusion composite sample can be normalized based upon the weight fractions and compositional properties of the bulk silane powder and surfactant added to the matrix epoxy to yield a value of 17.7 J/g, which implies that ~12.5% of the surfactant present in the initial bulk silane powder has phase-separated upon formation of the epoxy-silane IPN. It was not determined if the small amount of phase separation of the surfactant is occurring in the matrix phase or within the epoxy-silane IPN inclusions.

The network structures of the blends were also probed via DMA. Figures 7 and 8 show the E'' spectra in the temperature range of $-100–50$ °C for the neat matrix epoxy and particulate filled composite ($V_i = 0.49$), respectively. The broad low-temperature β-relaxation in the neat epoxy matrix (figure 7) is caused by the localized chair-to-boat conformational changes experienced in the cyclohexyl rings of the PACM curing agent (32). The α-relaxation of the epoxy-silane IPN, seen as the shoulders near $-10°$ in the E'' spectra of figure 8, is partially obscured by the β-relaxation of the matrix epoxy, which complicates the analysis of this data. The peaks observed near -60 °C in the E'' spectra of the particulate filled composite in figure 8 are presumable due to a small volume fraction of larger particles or agglomerations of particles of bulk silane powder, where diffusion of the matrix resin and curing agent was not completed and the formation of a homogeneous epoxy-silane IPN did not occur. Multiple frequency sweeps were used to resolve the peak shoulders embedded in the β relaxation E'' spectra of the matrix epoxy to characterize each contributing molecular relaxation mechanism. The α-relaxation (segmental motion) of the epoxy-silane IPN and the β-relaxation (short-range motion) of the glassy matrix epoxy will shift along the temperature (T) axis with varying extents as a function of frequency (f) due to differing Arrhenius activation energies (E_a) as defined by equation 18,

$$\log f = \frac{-E_a}{2.303R}\left(\frac{1}{T}\right).$$
(18)

Figure 7 illustrates the E'' spectra for the β-relaxation of the neat matrix epoxy as a function of temperature over three decades of frequency. The shape of the β-relaxation for the matrix epoxy is fairly symmetric, ranging from ~ -100 °C to nearly 50 °C, and does not change in shape as f is swept. The E_a value for the β-relaxation of the matrix epoxy was calculated to be equal to 63.7 kJ/mol, which is a typical value lying below 100 kJ/mol for secondary glassy motion (33). Figure 8 portrays the multiple low-temperature E'' relaxations present in the epoxy-silane IPN inclusion filled composite system. The overall shape of the E'' curves remains the same except for the presence of the low-temperature peak near -60 °C and a slight shoulder at -10 °C. The Arrhenius analysis yielded E_a values for these transitions of 226.7 and 366.2 kJ/mol for the low- and high-temperature transitions, respectively. Both transitions have E_a values greater than
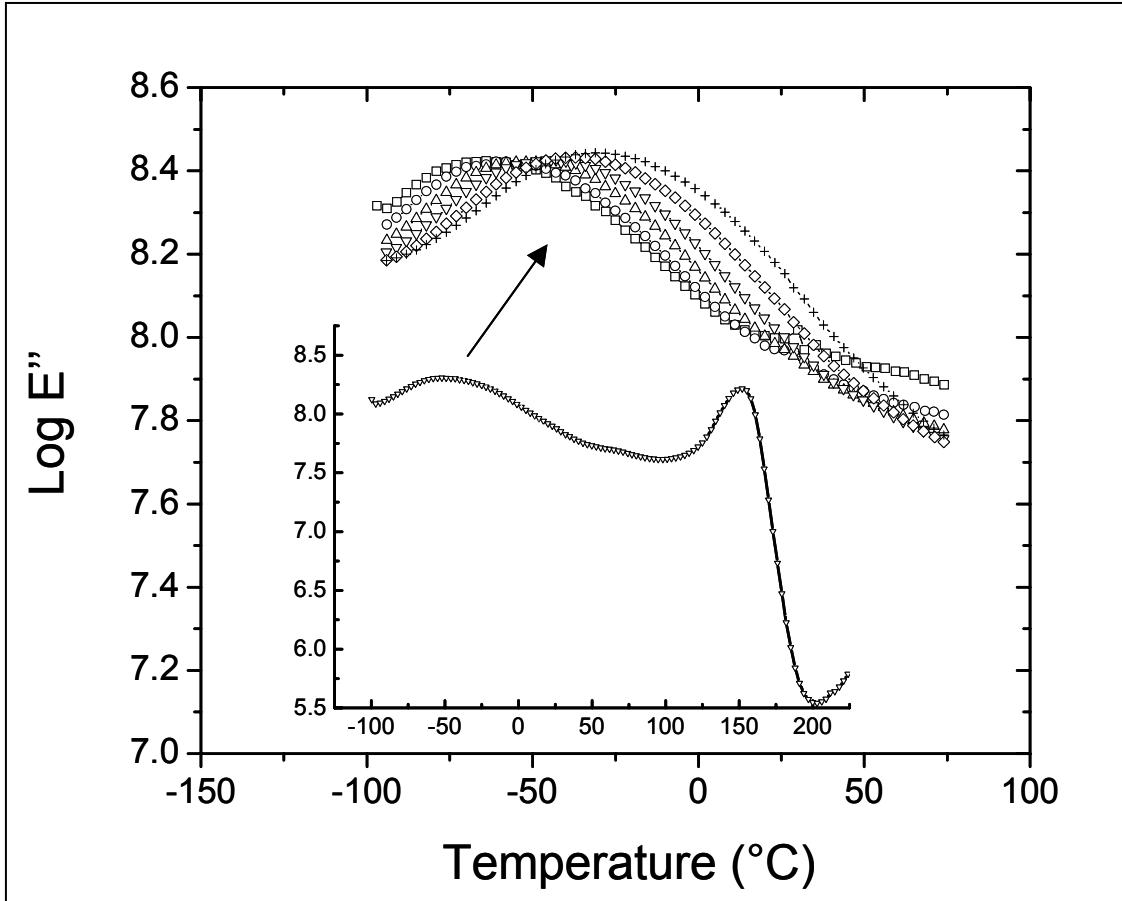
Figure 7. β-relaxation for neat epoxy matrix as measured by DMA as a function of temperature at constant frequency (□ = 0.1 Hz, ○ = 0.3 Hz, Î = 1 Hz, « = 3 Hz, ' = 10 Hz, + = 30 Hz).

100 kJ/mol, which is indicative of an α-transition. The Arrhenius plots are shown in figure 9. The α-transition seen as the shoulder at −60 °C could be the segmental relaxation of a small amount of unreacted silane powder within the matrix epoxy. Despite a generally good dispersion of particles some agglomeration was observed on the fracture surface SEM images. These agglomerates were too large to allow for complete diffusion of the epoxy resin and curing agent into the largest bulk silane particle prior to reaching the gel point of the matrix ($t_{diffusion} > t_{reaction}$). The α-transition shoulder at −10 °C corresponds to the fully reacted epoxy-silane IPN structure, as indicated by the increased value of T_g and E_a. Both the low- and high-temperature shoulder locations in the E'' spectra for the epoxy-silane IPN particulate filled composite sample observed via DMA are consistent with the transition temperatures trends obtained from DSC.

3.3   Quasi-Static Micromechanical Analysis

Figure 10 illustrates the quasi-static E_c vs. V_i plots for the particulate filled composites and the least squares fits to the rigorous C-Combining Rule (equation 1) as a function of temperature.

13
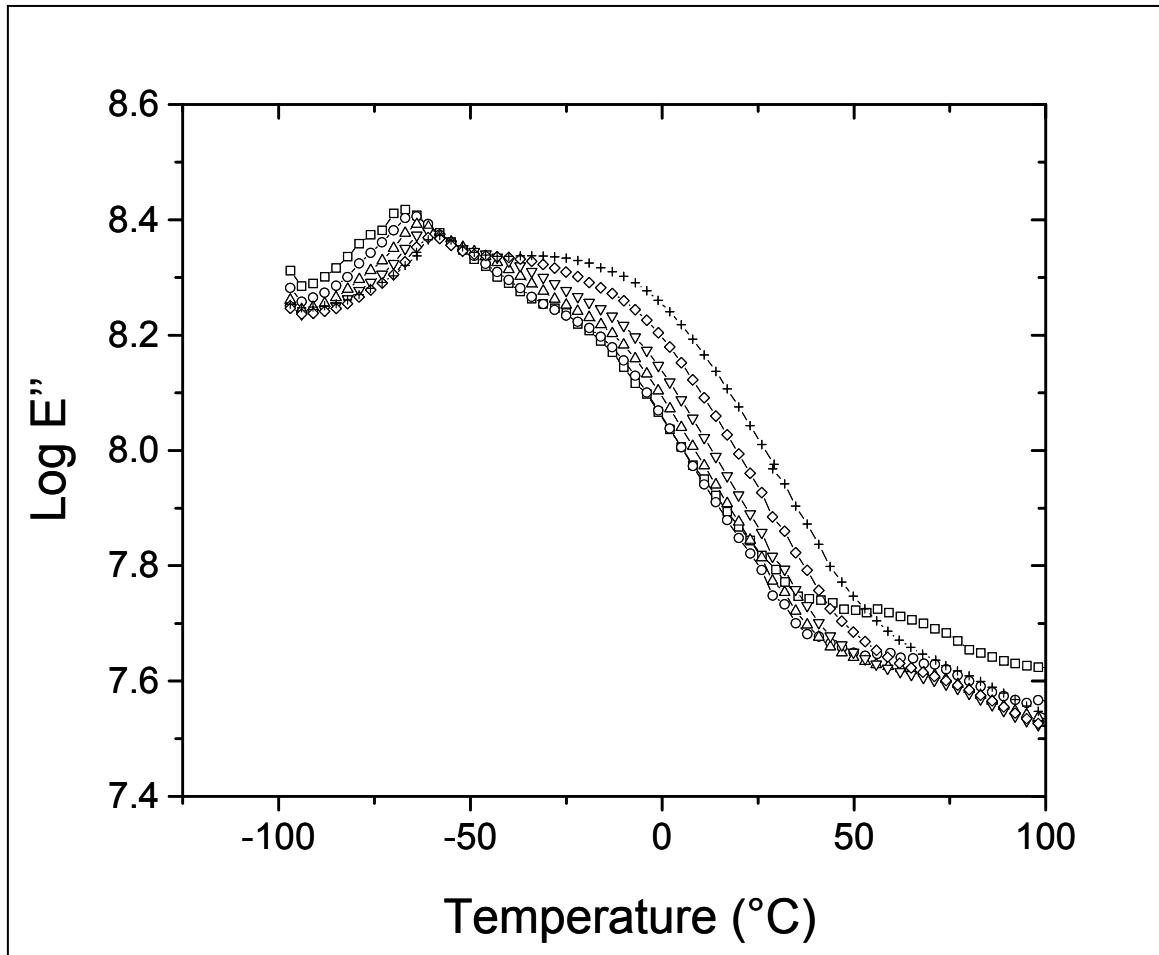
Figure 8. β-relaxation for epoxy-silane powder inclusion composite ($V_i = 0.49$) as measured by DMA as a function of temperature at constant frequency (□ = 0.1 Hz, ○ = 0.3 Hz, △ = 1 Hz, « = 3 Hz, ' = 10 Hz, + = 30 Hz).

The experimental data with error is listed in table 1. The extrapolated values of E_i were predicted using the E, G, and K conversion factors (equations 7 and 8), based on the assumption that $v_i = 1/3$ at T = −50 °C (glassy) and $v_i \sim 1/2$ at T = 25 and 100 °C (rubbery). For the matrix epoxy, v_m was assumed to equal 1/3 for the entire temperature range because at 100 °C the matrix epoxy is well below T_g and is still in the glassy state. Two observations are readily apparent from the data plotted in figure 10. The first prominent observation is that E_i is always less than E_m. The second observation is that the decrease in modulus for the epoxy-silane IPN inclusions upon transitioning from a glassy to a rubbery polymer at temperatures $T > T_g$ is small. Qualitatively, this relatively high rubbery modulus is indicative of a high value of ρ_c for the epoxy-silane IPN material. The DMA E' plots in the temperature range from −100 to 225 °C for the neat epoxy matrix and epoxy-silane IPN inclusion filled composite are illustrated in figure 11.
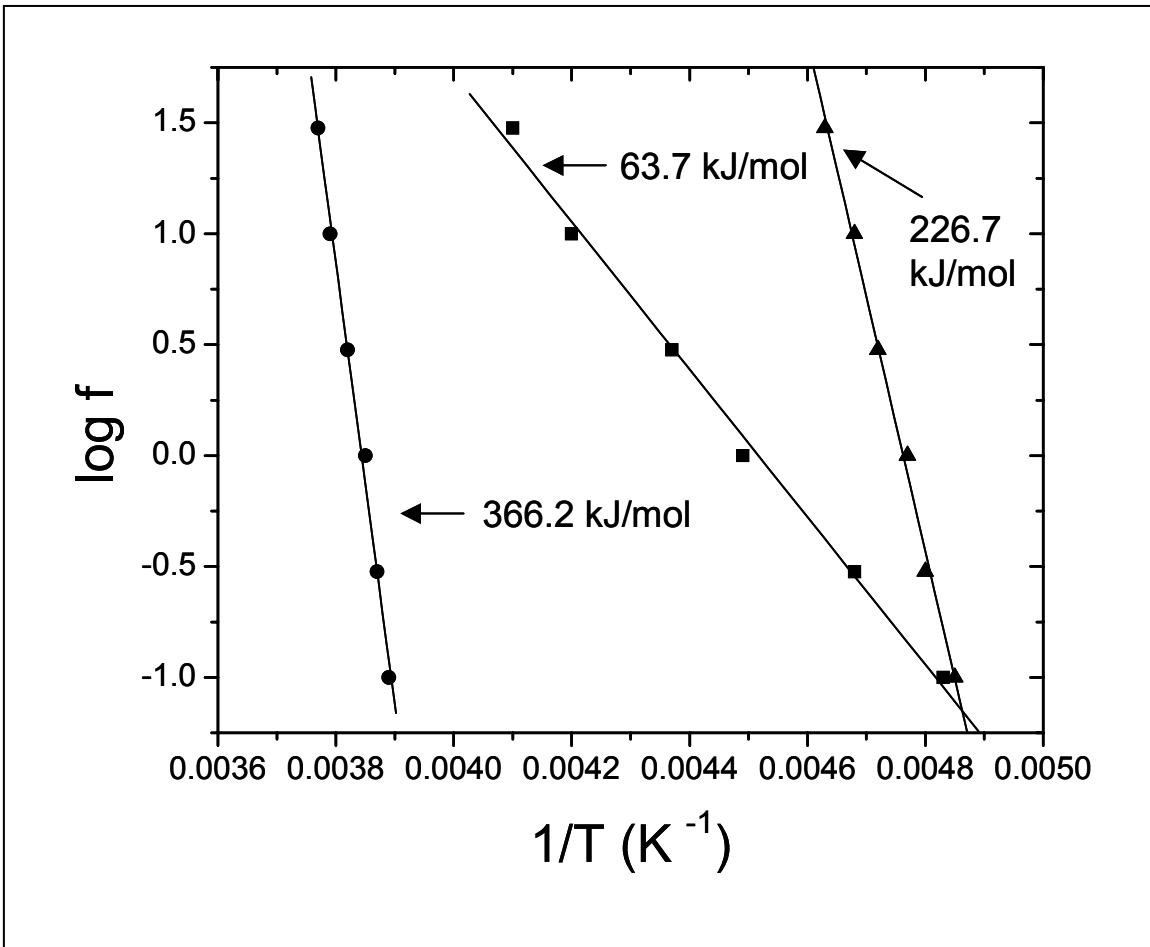
Figure 9. Arrhenius activation energies (equation 18) for the neat epoxy β-relaxation (■), nonreacted bulk silane powder α-transition (▲), and epoxy-silane IPN α-transition (●). Transition temperatures are taken from E'' spectra in figure 8.

The simplified exponential numerical approach (equation 12) for extrapolating to E_i at $V_i = 1$ was also tested using the quasi-static E_c data. These results are also summarized in table 1. The values of E_i estimated via equation 12 are in good agreement with those calculated rigorously using equation 1, differing by the greatest extent for the 100 °C data set. The exponential fit always predicts a slightly elevated value of E_i in comparison to the rigorous C-Combining Rule, due to the lack of a phase contiguity parameter. The exponential function was judged to provide an adequate approximation of the C-Combining Rule and was subsequently used to fit the dynamic modulus data.

3.4 Dynamic Modulus Analysis

The rationalization outlined in equations 14–16 is justified by the plots of the tan δ signals for the neat epoxy matrix and epoxy-silane IPN inclusion-filled composites illustrated in figure 12. In this plot, the region of interest is at subambient temperatures where the secondary β-relaxation of the matrix epoxy overlaps with the α-transition of the epoxy-silane IPN inclusions. The
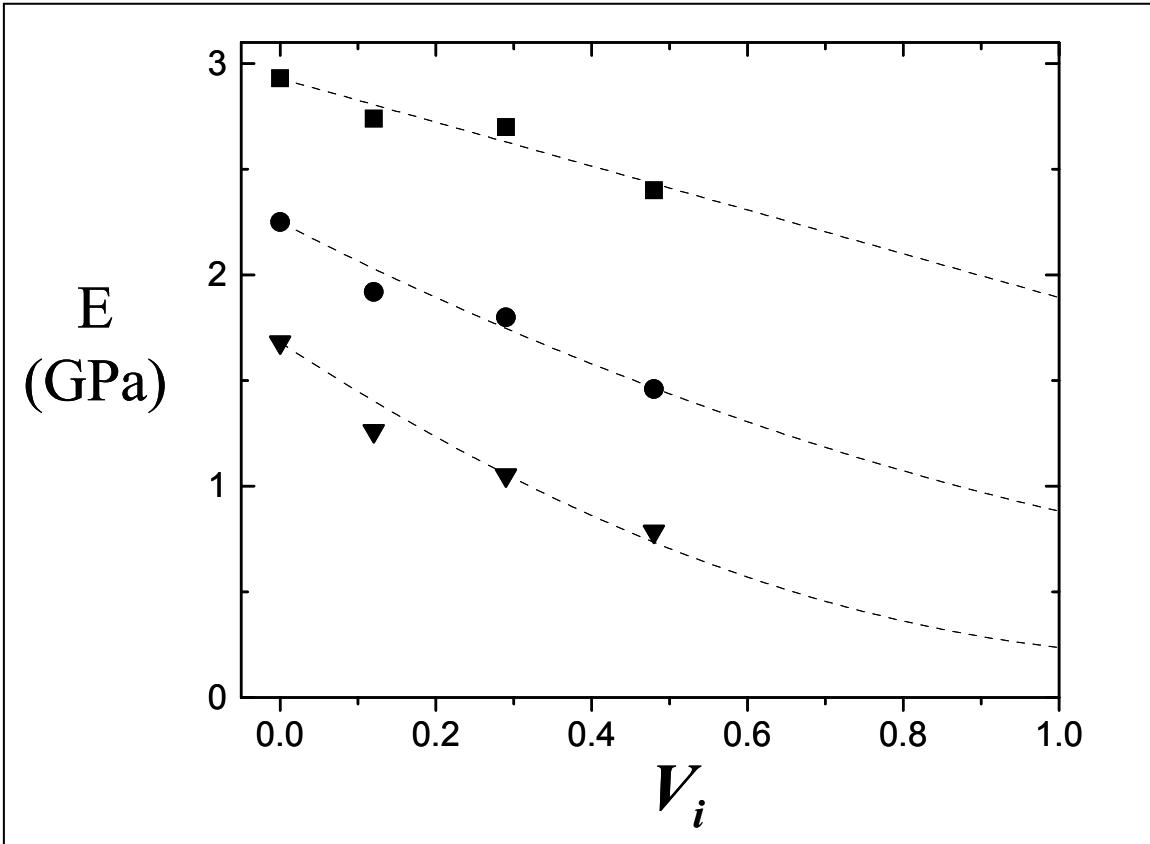
Figure 10. C-Combining Rule predictions of epoxy-silane IPN static modulus. Modulus values measured via experimental methodology outlined in ASTM D 790-96a. Experimental error was negligible, but is listed in table 1. (Test temperatures: ■ = −50 °C, ● = 25 °C, and ▲ = 100 °C.)

Table 1. Corresponding E values and error illustrated in figure 10.

V_i	E (GPa) T = −50 °C	E (GPa) T = 25 °C	E (GPa) T = 100 °C
0	2.93 (±0.05)	2.25 (±0.04)	1.68 (±0.07)
0.12	2.74 (±0.10)	1.92 (±0.04)	1.26 (±0.05)
0.30	2.70 (±0.06)	1.80 (±0.05)	1.05 (±0.02)
0.49	2.40 (±0.03)	1.46 (±0.03)	0.784 (±0.004)
1 [a]	1.89	0.89	0.24
1 [b]	1.99	0.93	0.33

[a]Predicted values obtained using the C-Combining Rule (equation 1).
[b]Predicted values using the exponential approximation function (equation 12).

α-transition of the matrix epoxy is present near 150 °C and is shown for reference. From these plots, it can be seen that both of the requirements for the low and balanced tan δ signal intensity are fulfilled, which warrants the ignoring of the imaginary component of the modulus equation 12. The mathematical rational for dropping the imaginary component of E^* can also be envisioned from a molecular structure point of view. Dickie (*28*) and Schapery (*29*) expressed
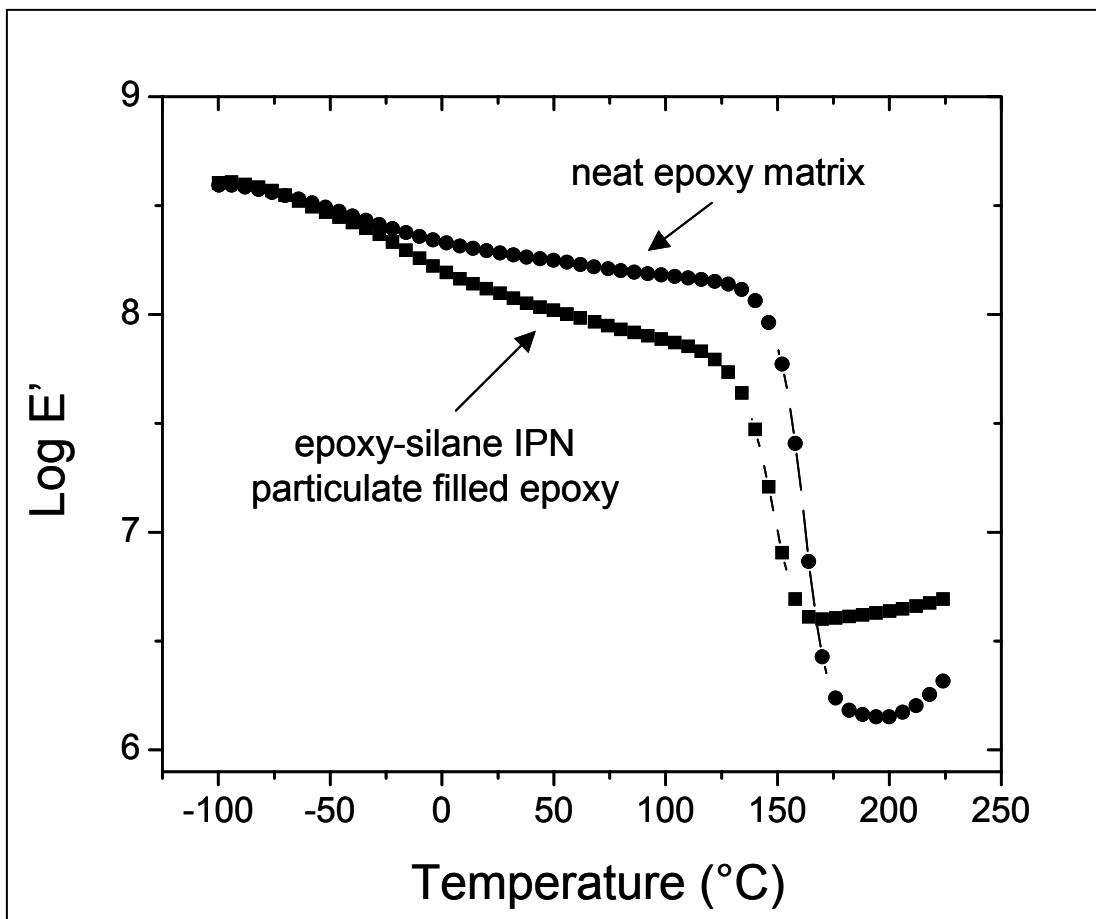
Figure 11. DMA E' plots comparing the neat epoxy matrix (●) and epoxy-silane IPN inclusion composite ($V_i = 0.49$, ■).

concern regarding the imaginary component of the dynamic modulus for situations where the α-transition of the inclusion occurs near the temperature range of the α-transition for the matrix. The physical and chemical interactions between the components of a polymer blend can lead to changes in the cooperative relaxation time scale of the α-transition for the individual constituents of the blend (*34, 35*). Furthermore, the alteration of the segmental relaxation of polymer blend components can also be a function of the blend composition (*36*). These variations in the time scale of the α-transitions of the blend components with volume fraction would result in inaccurate bounding values used to predict composite properties if the imaginary term of E^* is neglected. For the circumstance specifically presented in this research, the α-transition of the inclusion is superimposed upon the β-transition of the matrix. Fortunately, the molecular dynamics of the β-transition in polymer blends are localized and noncooperative, therefore remaining unaffected by compositional changes in the blend (*37–39*). Thus, the viscoelastic properties of the matrix epoxy were assumed to remain constant as a function of the epoxy-silane IPN inclusion concentration.
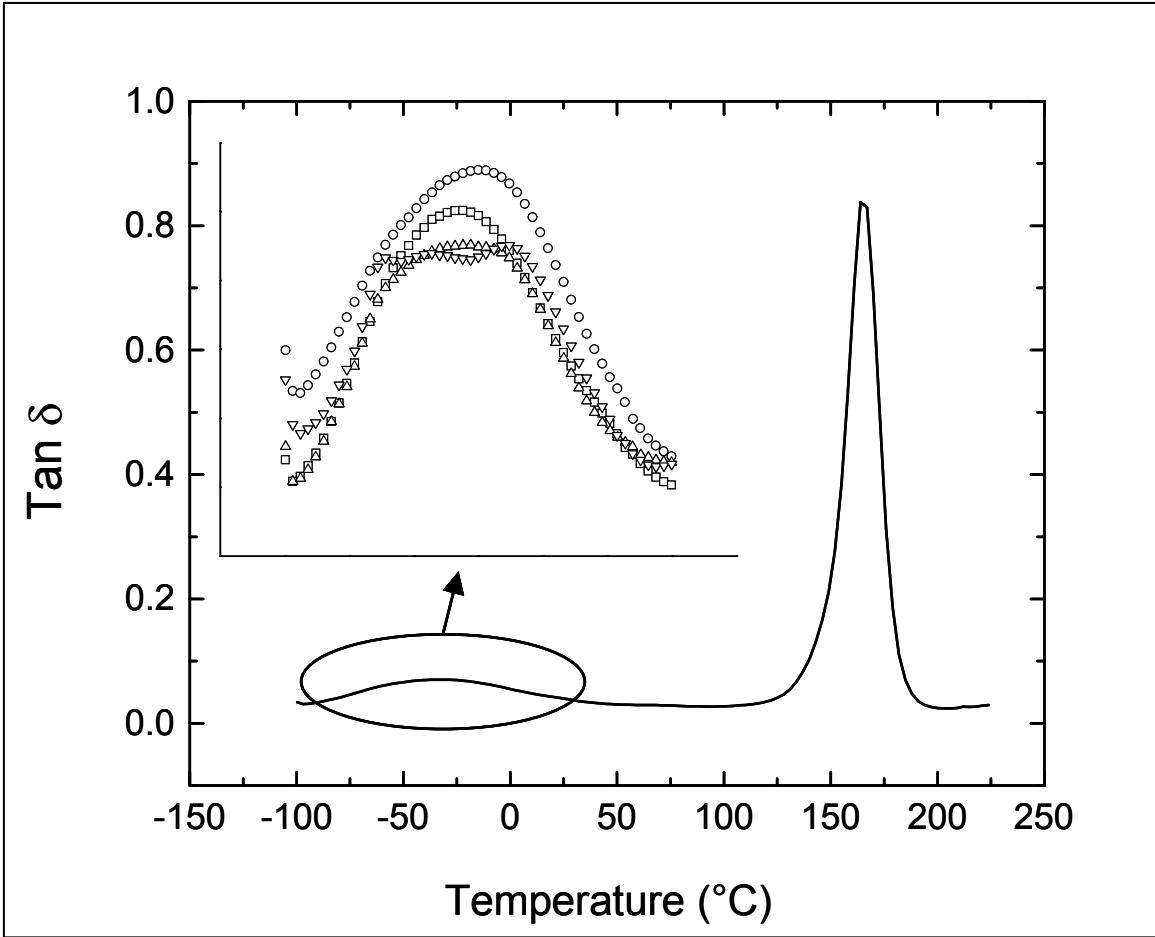
Figure 12. Tan δ signals measured from DMA. (□ = neat epoxy matrix, ○ = 0.12 volume % epoxy-silane IPN filler, Î = 0.29 volume % epoxy-silane IPN filler, « = 0.49 volume % epoxy-silane IPN filler).

The master curve obtained from the exponential determination (equation 12) of the epoxy-silane IPN inclusion modulus isotherms is portrayed in figure 13. The corresponding horizontal shift factor (a_T) plot for the master curve is shown in figure 14. The shift factor plot was also fit to the Williams-Landel-Ferry (WLF) equation, which is used to describe the temperature dependence of the distribution of relaxation times (*33*),

$$\log a_T = \frac{-C_1(T - T_0)}{C_2 + (T - T_0)}.$$

(19)

As can be seen in figure 14, the curvature of the experimental shift factor plot for the epoxy-silane IPN inclusions is well described by the WLF equation. The reference temperature (T_0) was set equal to T_g and a nonlinear least squares analysis yielded experimental C_1 and C_2 constants of 18.4 and 60.5/K, respectively. The experimental values determined for C_1 and C_2 are in good agreement with the universal values of 17.4 and 51.6/K, respectively. The shift factor plot also provided the opportunity to reevaluate the Arrhenius activation energy of the
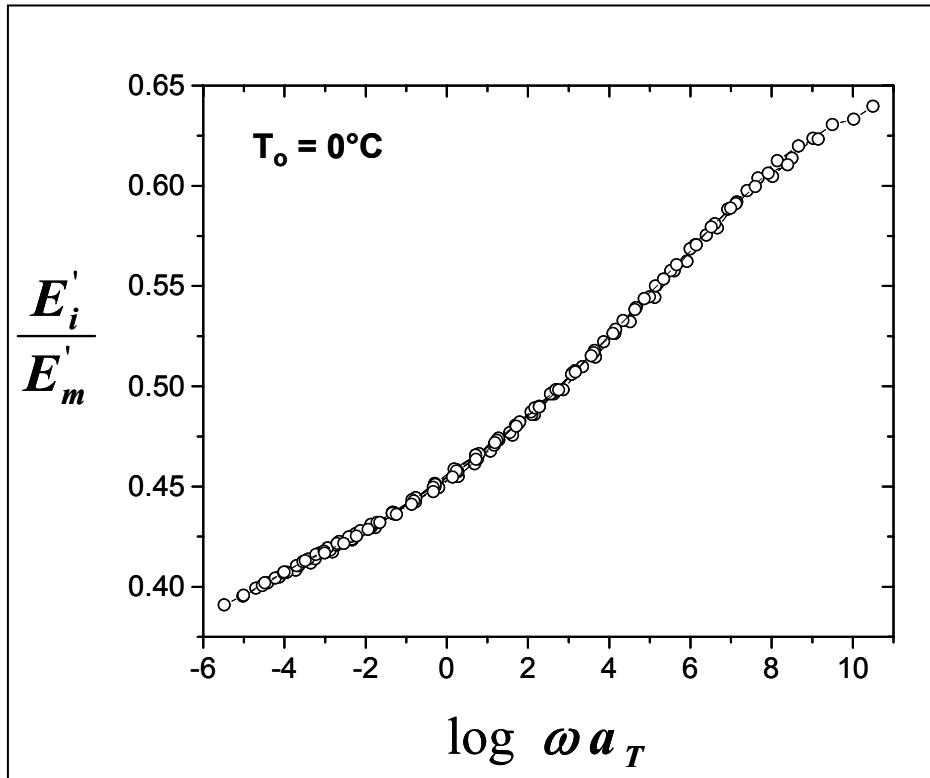
Figure 13. Experimental master curve for epoxy-silane IPN inclusions.

glass-to-rubber transition region for the epoxy-silane IPN inclusions through the following alternative expression for E_a:

$$E_a = 2.303R \left(\frac{d(\log a_T)}{d(1/T)} \right)_{T=T_0} .$$

(20)

Equation 20 generates a value of E_a equal to 371.2 kJ/mol in comparison to the value of 366.2 kJ/mol, which was obtained from the E'' plots shown in figure 8 and applying equation 18. These values are in excellent accord and place confidence in the accuracy of the master curve portrayed in figure 13.

3.5   Conversion of Modulus Ratio to Modulus Value

The preceding derivations were used to validate dropping the imaginary component of the dynamic modulus, the exponential fit (equation 12), and the vertical normalization scheme E_i/E_m used to construct the master curve illustrated in figure 13. The modulus ratios ensured that the empirical master curve is probably very accurate, but the values provided by E_i/E_m are not very useful for any future fiber-matrix interphase mechanical models. These modulus ratios need to be multiplied by E_m as to determine the actual magnitude of E_i. To facilitate this conversion of the modulus ratios another master curve of E' vs. frequency at $T_0 = 0$ °C for the neat matrix epoxy is required. The difficulty with constructing a master curve for the neat epoxy at $T_0 = 0$ °C

19
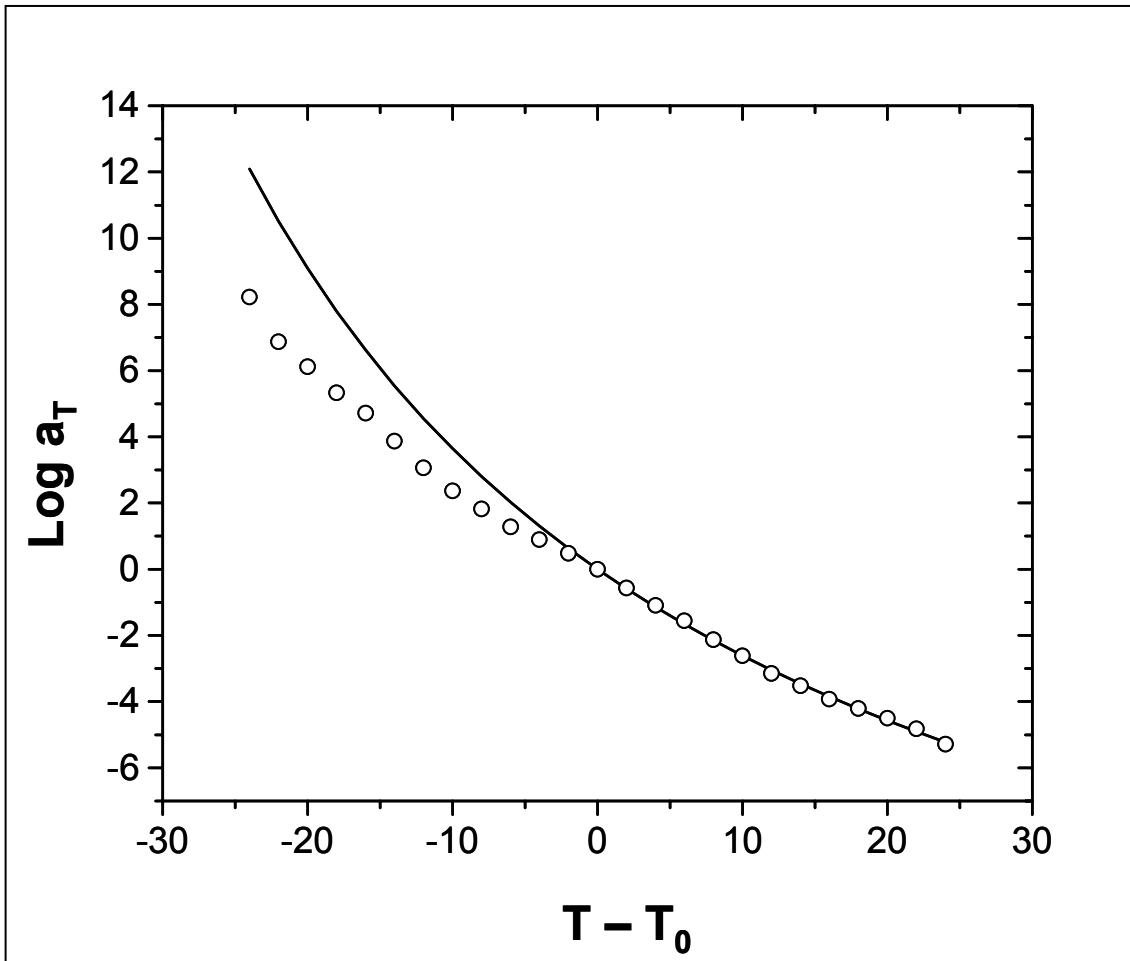
Figure 14. Shift factor plot (data points) for the epoxy-silane IPN inclusions with fit to WLF equation (solid line).

is that this reference temperature lies 155 °C below T_g, as seen in figure 11. Traditional time-temperature superposition fails in the glassy region of polymers due to the breakdown of the theory of rubber elasticity (*33*). The isothermal values of E' vs. frequency can be shifted in the β-relaxation region of a glassy polymer, but the vertical shift factor correction becomes extremely sensitive and the value of E_a determined via equation 20 will not match the experimental value determined from the multiple frequency sweep plots of E'' taken across the same temperature range (equation 18), which invalidates the master curve.

Simon and Ploehn (*40–42*) have recognized this issue and developed the tube-junction molecular model to successfully predict the isothermal modulus vs. frequency curves that will shift correctly in the glassy region of polymers. The tube-junction model balances the linear momentum of an axial (*a*) and transverse (*t*) polymer chain by considering the cohesive (F^c), entropic (F^s), and frictional (F^v) forces brought about by a dynamically induced stress,

$$F^c + F_a^s + F_s^t + F^v = 0 .$$ (21)

An in-depth discussion of the molecular dynamics and mathematical derivations governing the tube-junction model is beyond the scope of this report, but the premise behind the fitting of experimental data to the model is relatively straightforward. As discussed previously, confidence can be placed in the accuracy of a master curve if E_a obtained from the frequency sweep measurements matches the value calculated from the corresponding shift factor data taken after the construction of the master curve. Among the experimental parameters inputted into the tube-junction model are E_a and the breadth of the distribution for the β-relaxation. Basically, E_a for the β-relaxation of the neat epoxy matrix measured via the frequency dependence of the loss modulus is equal to 63.7 kJ/mol. Therefore, to ensure correlation, the frequency-dependent modulus predicted by the tube-junction model is assigned a value of E_a equal to 63.7 kJ/mol.

The storage and loss modulus vs. temperature curves ($f = 1$ Hz) as predicted by the tube-junction model are compared directly with the experimental DMA curves for the neat matrix epoxy in figure 15. The agreement between the experimental data and tube-junction model is excellent in the β-relaxation region. The agreement in the α-transition region is not as good, but this region is already adequately described by the WLF equation. Once a reasonable fit to the experimental data is found, the tube-junction model is used to predict multiple frequency sweep DMA data, and a master curve in the glassy region can be generated in normal fashion. The master curve for the neat epoxy at $T_0 = 0$ °C was then used to factor E_m from the E_i/E_m ratio used in figure 13. The E' master curves for the neat epoxy and the epoxy-silane IPN inclusions plotted on an absolute modulus scale are both portrayed in figure 16. The storage modulus for the epoxy-silane IPN ranges from ~3 GPa to 750 MPa in the glassy and rubbery response regions, respectively. The modulus of the epoxy-silane IPN is always lower in comparison to the neat epoxy matrix, which ranges from ~4.75 GPa to 1.75 GPa over the same frequency range.

4. Conclusions

To elucidate the typical properties of a silane-modified interphase, the structure of an organofunctional silane/thermoset crosslinked IPN was studied. A model epoxy-silane IPN was synthesized to simulate the molecular structure found at a representative silane-epoxy-glass fiber-matrix interphase. Bulk silane was hydrolyzed and condensed in the presence of a surfactant and epoxy film former to mimic commercial glass fiber sizings in larger and more easily characterized samples. The resulting material consisted of a powder with a T_g of −50 °C. The model bulk silane powder was next mixed at varied volume fractions in an epoxy matrix to form filled composites in which spherical particulates of epoxy-silane IPN material formed the inclusion phase. Several important results were obtained. First, the diffusion and reaction of the epoxy-amine matrix resin into the bulk silane powder resulted in a significant increase in the T_g of the particulate upon formation of the epoxy-silane IPN. This was due to the additional
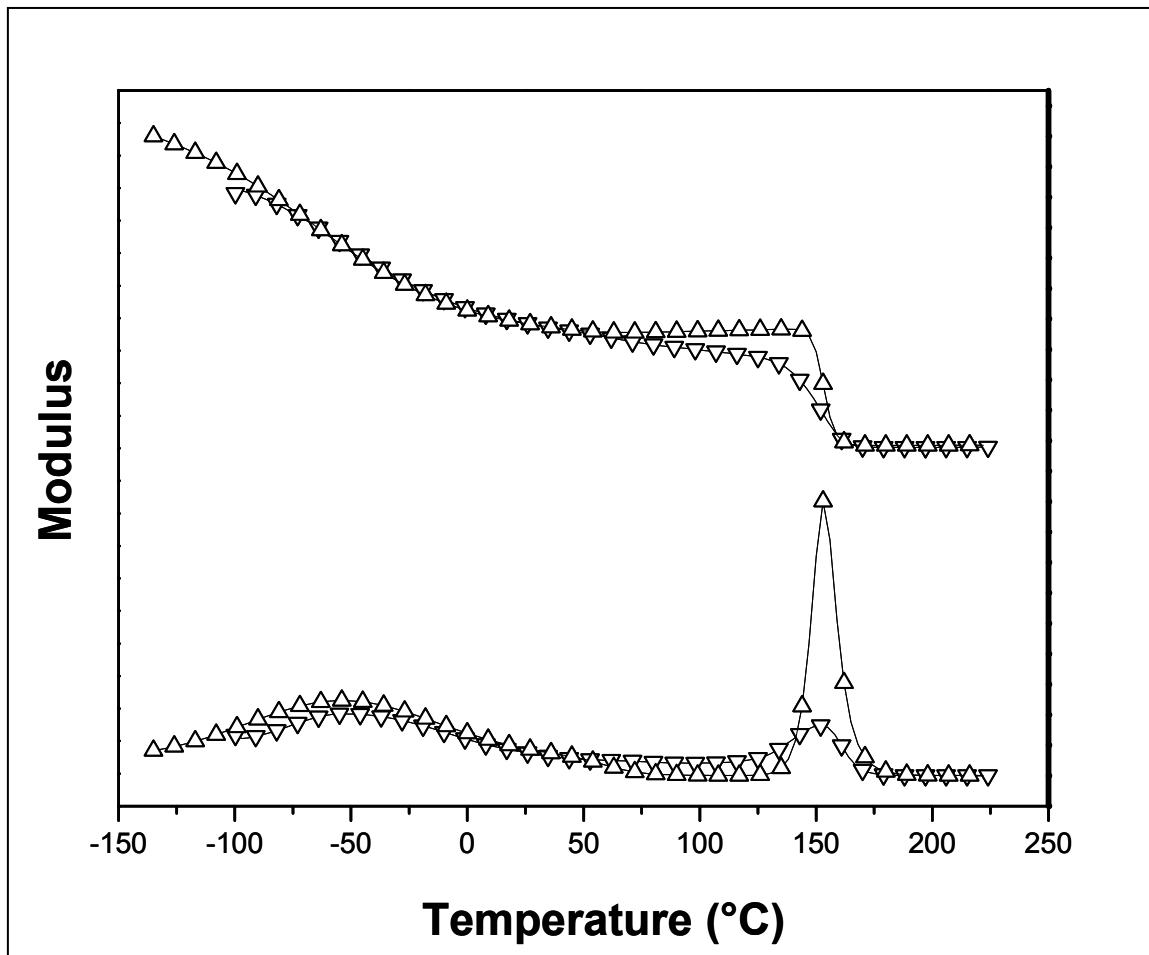
Figure 15. Comparison of modulus plots between experimental DMA (1-Hz) data and those predicted from the tube-junction model. Fitting parameters were K = 2.5 GPa, ε = 0.0006, μ = 63.7 kJ/mol, σ = 12 kJ/mol, Z = 60 kJ/mol, and T_g = 370 K. All other fitting parameters needed for the tube-junction model were kept identical, as cited by Simon and Ploehn (*40*). ($\ll$ = experimental data, and $\hat{\mathrm{I}}$ = tube-junction model.)

crosslinking of the matrix resin's curing agent with the epoxy functional groups in the bulk silane powder, as well as possible infusion and crosslinking with additional matrix epoxy resin. This T_g of the epoxy-silane IPN was still significantly lower than that of the neat epoxy matrix (0 vs. 155 °C), suggesting that a similar interphase in a composite would also have a lower T_g. Hence the mechanical response of the interphase would be significantly different than the bulk as was expected.

Next, to quantify the mechanical properties of the epoxy-silane IPN inclusions embedded in the epoxy matrix, a micromechanical analysis was devised to determine the properties of the inclusion through measurements obtained on particulate filled composite specimens. Specifically, the C-Combining Rule was applied to data obtained under quasi-static conditions to predict the epoxy-silane IPN modulus based upon the overall composite and constituent matrix
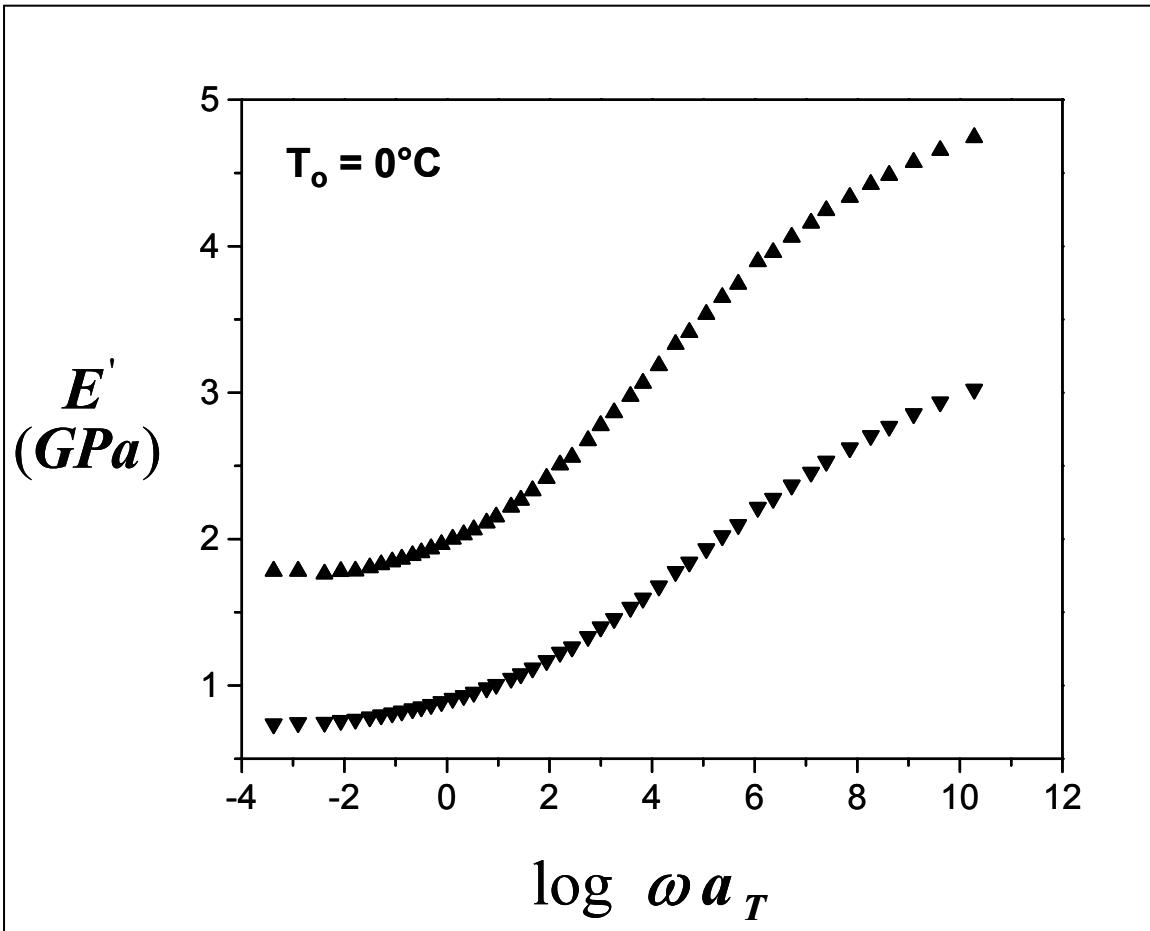
Figure 16. Corrected master curves for matrix epoxy (▲) and epoxy-silane IPN inclusions (▼).

properties. These results show that the modulus of the epoxy-silane IPN was always lower than the modulus of the epoxy matrix and, not surprisingly, this difference was greatest when the test temperature was much greater than the epoxy-silane IPN T_g ($T >> 0$ °C). The rate-dependent storage modulus of the model epoxy-silane IPN was determined using appropriate viscoelastic micromechanical descriptions developed for this study and shown to differ greatly from the matrix response at all temperatures and rates.

This study has attempted to quantify the properties of a specific epoxy-silane IPN that are typical of those found at silane-modified interphases of glass-reinforced composites. Although possible effects to the model epoxy-silane IPN due to the fiber surface (e.g., restriction to the molecular mobility, preferential adsorption of curing agent or resin, variations in ρ_c, entropic effects, etc.) are conveniently absent, these results indicate the importance of considering the properties of the epoxy-silane IPN interphase. The findings are expected to have relevance to efforts that seek to model the interphase-dependent mechanical response of composites including impact, fatigue and durability. Furthermore, the methods described in this work may be used to help design interphase materials with desired thermal and mechanical properties.

5. References

1. Plueddemann, E. P. *Silane Coupling Agents,* 2nd Ed.; Plenum Press: New York, 1990.

2. Hoh, K. P.; Ishida, H.; Koenig, J. L. *Polym Comp.* **1988**, *9* (2), 151.

3. Drown, E. K.; Almoussawi, H.; Drzal, L. T. *J. Adh. Sci. Tech*. **1991**, *5* (10), 865.

4. Suryanarayana, D.; Mittal, K. L. *J. Appl. Polym. Sci*. **1984**, *29* (6), 2039.

5. Dillingham, R. G.; Boerio, F. J. *J. Adh. Sci. Tech*. **1992**, *6* (1), 207.

6. Tesoro, G.; Wu, Y. L. *J. Adh. Sci. Tech*. **1991**, *5* (10), 771.

7. Bayer, T.; Eichhorn, K. J.; Grundke, K.; Jacobasch, H. *J. Macromol. Chem. Physic*. **1999**, *200* (4), 852.

8. Wang, D.; Jones, F. R. *Comp. Sci. Tech*. **1994**, *50* (2), 215.

9. Mader, E.; Pisanova, E. *Macromolecular Symposia* **2001**, *163*, 189–212.

10. Dibenedetto, A. T. *Mat. Sci. Eng. Part A* **2001**, *302* (1), 74.

11. Connell, M. E.; Cross, W. M.; Snyder, T. G.; Winter, R. M.; Kellar, J. *J. Comp. Part A* **1998**, *29* (5–6), 495.

12. Gentle, T. E.; Schmidt, R. G.; Naasz, B. M.; Gellman, A. J.; Gentle, T. M. *J. Adh. Sci. Tech*. **1992**, *6* (2), 307.

13. Madhukar, M. S.; Drzal, L. T. *J. Comp. Mat*. **1991**, *25* (8), 932.

14. Madhukar, M. S.; Drzal, L. T. *J. Comp. Mat*. **1991**, *25* (8), 958.

15. Lesko, J. J.; Swain, R. E.; Cartwright, J. M.; Chin, J. W.; Reifsnider, K. L.; Dillard, D. A.; Wightman, J. P. *J. Adhesion* **1994**, *45* (1–4), 43.

16. Reifsnider, K. L. *Composites* **1994**, *25* (7), 461.

17. Hartman, D. R.; Jutte, R. B.; Beaver, T. R.; Hill, H. G. United States Patent 5,006,293, 1991.

18. Tanoglu, M.; McKnight, S. H.; Palmese, G. R.; Gillespie, J. W. *Comp. Sci. Tech*. **2001**, *61* (2), 205.

19. Van Landingham, M. R.; Dagastine, R. R.; Eduljee, R. F.; McCullough, R. L.; Gillespie, J. W. *Comp. Part A* **1999**, *30* (1), 75.

20. Bogetti, T. A.; Wang, T.; Van Landingham, M. R.; Gillespie, J. W. *Comp. Part A* **1999**, *30* (1), 85.

21. Verghese, K. N. E.; Jensen, R. E.; Lesko, J. J.; Ward, T. C. *Polymer* **2001**, *42* (4), 1663.

22. Tanoglu, M.; Ziaee, S.; McKnight, S. H.; Gillespie, J. W.; Palmese, G. P. *J. Mat. Sci.* **2001**, *36* (12), 3041–3053.

23. Cowie, J. M. G. *Polymers: Chemistry and Physics of Modern Materials,* 2nd Ed.; Blackie Academic & Professional: New York, NY, 1991.

24. Thomason, J. L. *Composites* **1995**, *26* (7), 487.

25. ASTM D 790-96a. Standard Test Methods for Flexural Properties of Unreinforced and Reinforced Plastics and Electrical Insulating Materials. *Annu. Book ASTM Stand.* **1998**.

26. Whitney, J. M.; McCullough, R. L. *Delaware Composites Design Encyclopedia*, Vol. 2; Technomic: Lancaster, PA, 1990.

27. Hashin, Z.; Shtrikman, S. *J. Mech. Phys. Solids* **1963**, *11*, 127.

28. Dickie, R. A. *J. Appl. Polym. Sci.* **1973**, *14*, 45.

29. Schapery, R. A. *Mechanics of Composite Materials*, Vol. 2; Sendeckyj, G. P., Ed.; Academic Press: New York, NY, 1974.

30. Gorowara, R. L.; Kosik, W. E.; McKnight, S. H.; McCullough, R. L. *Comp. Part A* **2001**, *32*, 323.

31. Palmese, G. R.; McCullough, R. L. *J. Appl. Polym. Sci.* **1992**, *46* (10), 1863.

32. Eichstadt, A. E.; Bagwell, M.; Dunson, D.; McGrath, J. E.; Ward, T. C. *Proceedings of the 24th Annual Meeting of the Adhesion Society*, Williamsburg, VA; The Adhesion Society: Blacksburg, VA; **2001**, *24*, 119.

33. Ferry, J. D. *Viscoelastic Properties of Polymers,* 2nd Ed.; Wiley & Sons: New York, NY, 1970.

34. Sy, J. W.; Mijovic, J. *Macromolecules* **2000**, *33*, 933.

35. Sanchis, A.; Prolongo, M. G.; Masegosa, R. M.; Rubio, R. G. *Macromolecules* **1995**, *28*, 2693.

36. Dionisio, M.; Fernandes, A. C.; Mano, J. F.; Correia, N. T.; Sousa, R. C. *Macromolecules* **2000**, *33*, 1002.

37. Bristow, J. F.; Kalika, D. S. *Macromolecules* **1994**, *27*, 1808.

38. Cendoya, I.; Alegria, A.; Alberdi, J. M.; Colmenero, J.; Grimm, H.; Richter, D.; Frick, B. *Macromolecules* **1999**, *32*, 4065.

39. Arbe, A.; Alegria, A.; Colmenero, J.; Hoffmann, S.; Willner, L.; Richter, D. *Macromolecules* **1999**, *32*, 7572.

40. Simon, P. P.; Ploehn, H. J. *J. Rheol.* **1997**, *41*, 641.

41. Simon, P. P.; Ploehn, H. J. *J. Appl. Polym. Sci. Part B* **1999**, *37*, 127.

42. Simon, P. P.; Ploehn, H. J. *J. Rheol.* **2000**, *44*, 169.

Appendix. Explicit Inclusion Modulus Determination

The use of micromechanical bounding models to "back-out" an unknown modulus of a particulate inclusion by extrapolating to $V_i = 1$ is actually incorrect. For example, a least squares fit of an arbitrary set of composite property (P_c) vs. V_i data to the simple Reuss lower bound ($1/P_c = V_m / P_m + V_i / P_i$) and Voigt upper bound ($P_c = V_m P_m + V_i P_i$) models readily exemplifies the error with this analysis route. As can be seen in figure A-1, a least squares fit is forcing the data to assume the curvature of the model of choice and the lower bound model will wrongly predict a higher value of inclusion modulus than the upper bound model. To avoid this dilemma in analysis, the inclusion modulus of a particulate filled composite must be determined explicitly using the combining rules at each value of V_i. It can also be shown, after much derivation, that any combining rule can be used to express the ratio E_c/E_m in the following algebraic equation:

$$\left(\frac{E_c}{3E_m}\right) n_k F_k + \left(\frac{E_c}{3E_m}\right) n_G F_G - F_k F_G = 0, \tag{A-1}$$

where

$$n_k, n_G, F_G, F_k = f(E_i, \nu_i, \nu_m, V_i, V_m). \tag{A-2}$$

The input parameters for equation A-1 can all be determined experimentally with the exception of ν_i, ν_m, and E_i. If the values of Poisson's ratio for the matrix and inclusion are assumed then the terms of equation A-1 can be rearranged to solve for E_i. The solution to the C-Combining Rule using equation A-1 yields a 3rd order polynomial with 2 negative roots and 1 positive root. The isothermal E_c/E_m data at $V_i = 0.49$ was used to reevaluate the epoxy-silane interpenetrating network (IPN) inclusion master curve illustrated in figure 13, using the rigorous format of equation A-1. For the calculations of the new isothermal data, ν_m was assumed to equal a constant value of 1/3 for all values of T, and ν_i was set equal to 1/3 at $T < T_g$ and 1/2 at $T > T_g$. The new rigorous modulus isotherms were then shifted horizontally along the frequency axis using the a_T values plotted in figure 14 to form a new master curve, which is illustrated in figure A-2. Several key results can be observed from the rigorous master curve. The assumptions made pertaining to ν_i are valid only in the glassy and rubbery plateau regions where the modulus isotherms were shifted successfully using the a_T values transposed from figure 14. Poisson's ratio is the key-driving factor in equation A-1, and the lack of reasonable approximations of ν_i in the glass transition region causes the abrupt discontinuity in the rigorous master curve. The simplified exponential fit (equation 12) is unbiased by Poisson's ratio in the glass transition region, which is why the empirical master curve shown in figure 13 is smooth and continuous. The magnitudes of the predicted modulus ratios are also in good agreement between the
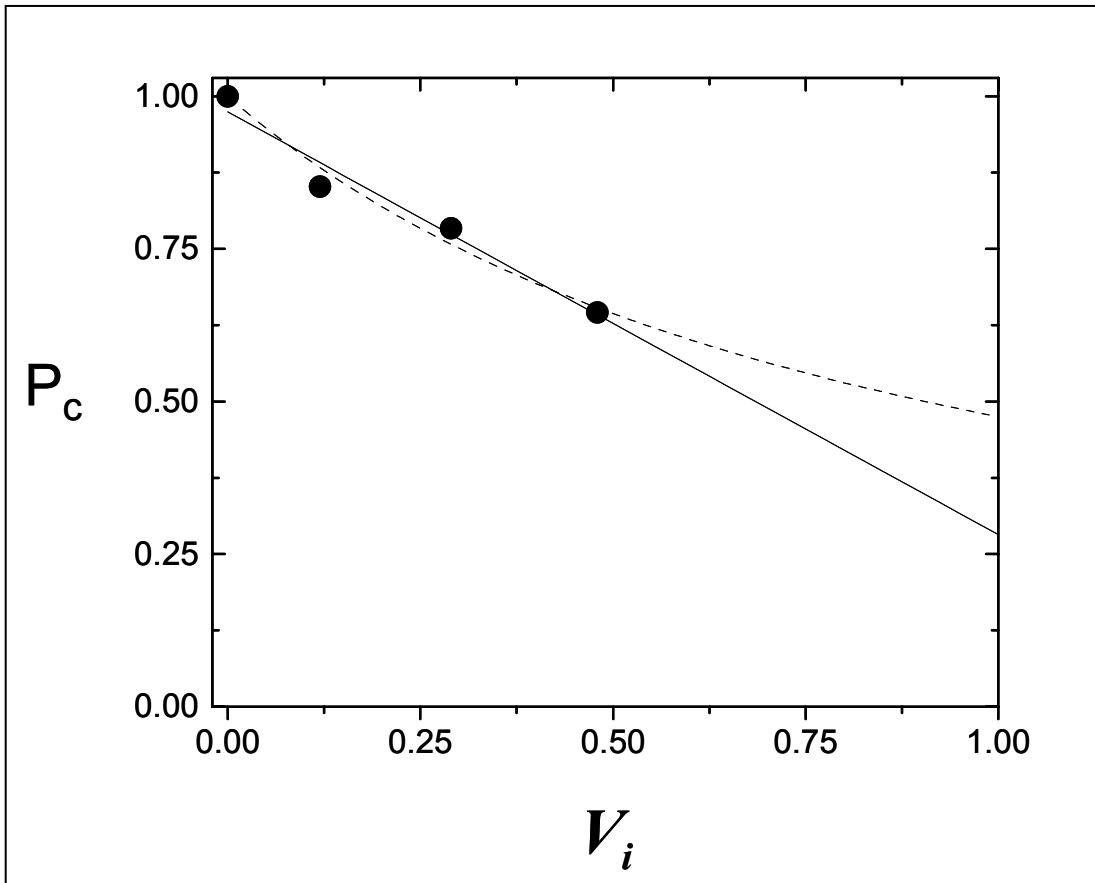
Figure A-1. Arbitrary data set fit to the Voigt upper (solid line) and Reuss lower (dashed line) bound
predictions using a least squares regression.

empirical and rigorous master curves. However, the rigorous master curve does expectedly
predict slightly lower values of E_i/E_m in the rubbery plateau region due to phase contiguity
parameter of the C-Combining Rule. It is also interesting to note that if the difference in
magnitude between the rubbery and glassy modulus of the epoxy-silane IPN inclusions were
greater then the error due to the simplified exponential fit and extrapolation procedure, used to
derive the master curve in figure 13, would have potentially become much greater.
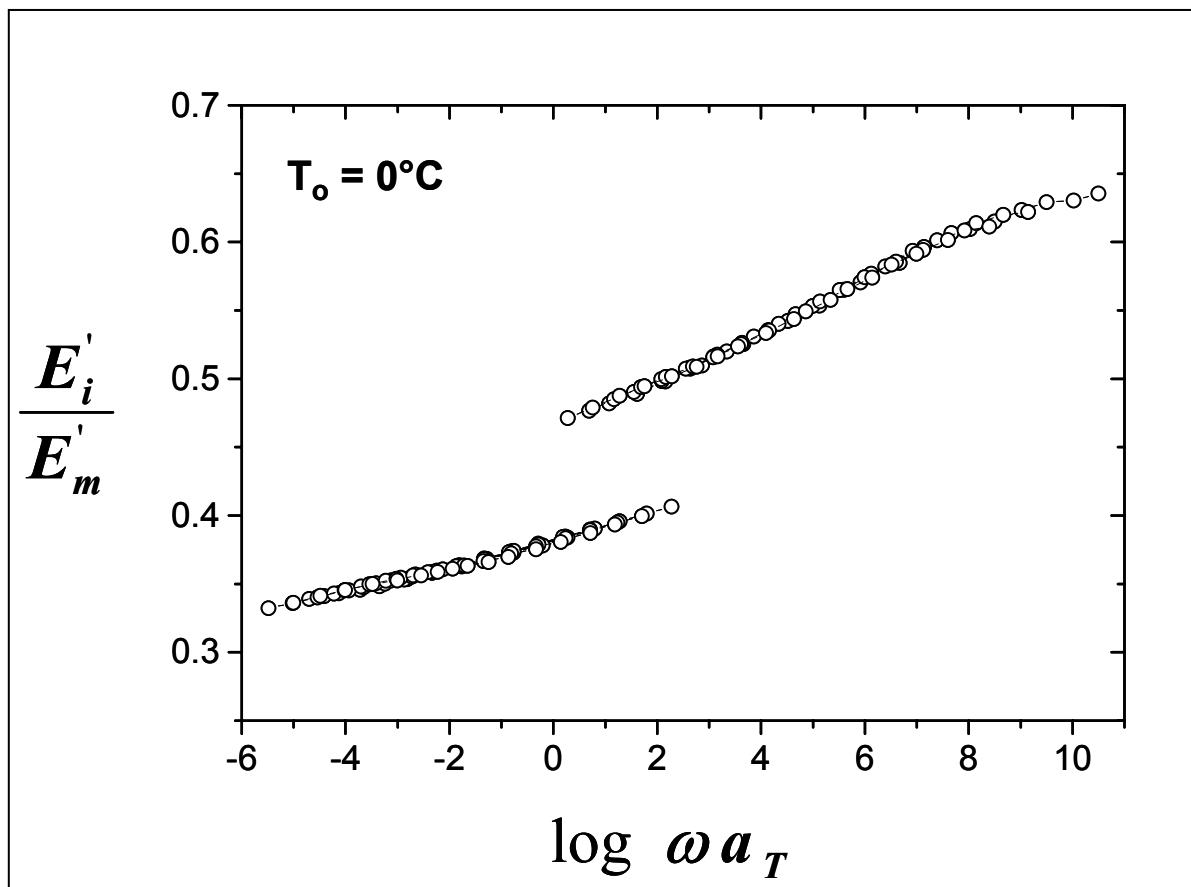
Figure A-2. Rigorous master curve obtained from the C-Combining Rule using equation 22. Isotherms were shifted using identical a_T values as used in figure 14.

NO. OF
COPIES   ORGANIZATION

1*   DEFENSE TECHNICAL
     INFORMATION CENTER
     DTIC OCA
     8725 JOHN J KINGMAN RD
     STE 0944
     FT BELVOIR VA 22060-6218

1   COMMANDING GENERAL
     US ARMY MATERIEL CMD
     AMCRDA TF
     5001 EISENHOWER AVE
     ALEXANDRIA VA 22333-0001

1   INST FOR ADVNCD TCHNLGY
     THE UNIV OF TEXAS
     AT AUSTIN
     3925 W BRAKER LN STE 400
     AUSTIN TX 78759-5316

1   US MILITARY ACADEMY
     MATH SCI CTR EXCELLENCE
     MADN MATH
     THAYER HALL
     WEST POINT NY 10996-1786

1   DIRECTOR
     US ARMY RESEARCH LAB
     AMSRD ARL D
     DR D SMITH
     2800 POWDER MILL RD
     ADELPHI MD 20783-1197

1   DIRECTOR
     US ARMY RESEARCH LAB
     AMSRD ARL CS IS R
     2800 POWDER MILL RD
     ADELPHI MD 20783-1197

3   DIRECTOR
     US ARMY RESEARCH LAB
     AMSRD ARL CI OK TL
     2800 POWDER MILL RD
     ADELPHI MD 20783-1197

3   DIRECTOR
     US ARMY RESEARCH LAB
     AMSRD ARL CS IS T
     2800 POWDER MILL RD
     ADELPHI MD 20783-1197

NO. OF
COPIES   ORGANIZATION

ABERDEEN PROVING GROUND

2   DIR USARL
     AMSRD ARL CI LP (BLDG 305)
     AMSRD ARL CI OK TP (BLDG 4600)

---

* PDF only.

NO. OF COPIES	ORGANIZATION
1	DIRECTOR US ARMY RESEARCH LAB AMSRL CI IS R 2800 POWDER MILL RD ADELPHI MD 20783-1145
3	DIRECTOR US ARMY RESEARCH LAB AMSRL OP SD TL 2800 POWDER MILL RD ADELPHI MD 20783-1145
1	DPTY ASST SECY FOR R&T SARD TT THE PENTAGON RM 3EA79 WASHINGTON DC 20301-7100
1	COMMANDER US ARMY MATERIEL CMD AMXMI INT 5001 EISENHOWER AVE ALEXANDRIA VA 22333-0001
2	USA SBCCOM MATERIAL SCIENCE TEAM AMSSB RSS J HERBERT M SENNETT KANSAS ST NATICK MA 01760-5057
1	US ARMY SBCCOM SOLDIER SYSTEMS CENTER BALLISTICS TEAM W ZUKAS KANSAS ST NATICK MA 01760-5019
2	US ARMY RESEARCH OFC D STEPP D KISEROW PO BOX 12211 RESEARCH TRIANGLE PARK NC 27709-2211
2	NAVAL SURFACE WARFARE CTR CARDEROCK DIVISION R CRANE CODE 6553 C WILLIAMS CODE 6553 9500 MACARTHUR BLVD WEST BETHESDA MD 20817-5000

NO. OF COPIES	ORGANIZATION
2	AFRL F ABRAMS J BROWN BLDG 653 2977 P ST STE 6 WRIGHT PATTERSON AFB OH 45433-7739
1	OAK RIDGE NATIONAL LABORATORY C EBERLE MS 8048 PO BOX 2008 OAK RIDGE TN 37831
1	NASA LANGLEY RSCH CTR AMSRL VS W ELBER MS 266 HAMPTON VA 23681-0001
1	UNIVERSITY OF DELAWARE CNTR FOR COMPOSITE MATERIALS G PALMESE NEWARK DE 19716

ABERDEEN PROVING GROUND

NO. OF COPIES	ORGANIZATION
1	DIRECTOR US ARMY RESEARCH LAB AMSRL OP AP L APG MD 21005-5066

9	DIR USARL
	AMSRL CS IO FI
	  M ADAMSON
	AMSRL WM
	  J SMITH
	  J MCCAULEY
	AMSRL WM B
	  A HORST
	AMSRL WM MA
	  R JENSEN (2 CPS)
	  S MCKNIGHT
	AMSRL WM M
	  B FINK
	AMSRL WM T
	  B BURNS

INTENTIONALLY LEFT BLANK.